

Journal of Visualized Experiments

Optocardiography and Electrophysiology Studies of Ex Vivo Langendorff-Perfused Pig Hearts

--Manuscript Draft--

Article Type:	Invited Methods Article - JoVE Produced Video
Manuscript Number:	JoVE60472R2
Full Title:	Optocardiography and Electrophysiology Studies of Ex Vivo Langendorff-Perfused Pig Hearts
Section/Category:	JoVE Biology
Keywords:	fluorescence, imaging, electrophysiology, heart, electrocardiogram, optical mapping, optocardiography
Corresponding Author:	Nikki Posnack Children's National Health System Washington, DC UNITED STATES
Corresponding Author's Institution:	Children's National Health System
Corresponding Author E-Mail:	NPOSNACK@childrensnational.org
Order of Authors:	Luther Swift Rafael Jaimes Damon McCullough Morgan Burke Takuya Maeda Hanyu Zhang Nobuyuki Ishibashi Jack M Rogers Nikki Posnack
Additional Information:	
Question	Response
Please indicate whether this article will be Standard Access or Open Access.	Open Access (US\$4,200)
Please indicate the city, state/province, and country where this article will be filmed . Please do not use abbreviations.	Washington, DC, USA

TITLE:**Optocardiography and Electrophysiology Studies of Ex Vivo Langendorff-Perfused Pig Hearts****AUTHORS AND AFFILIATIONS:**

Luther M. Swift^{1,2}, Rafael Jaimes III^{1,2}, Damon McCullough^{1,2}, Morgan Burke^{1,2}, Marissa Reilly^{1,2}, Takuya Maeda^{1,2,3}, Hanyu Zhang⁴, Nobuyuki Ishibashi^{1,2,3}, Jack M. Rogers⁴, Nikki Gillum Posnack^{1,2,5}

¹Sheikh Zayed Institute for Pediatric and Surgical Innovation: Children's National Health System, Washington DC, USA

²Children's National Heart Institute: Children's National Health System, Washington DC, USA

³Center for Neuroscience Research: Children's National Health System, Washington DC, USA

⁴Department of Biomedical Engineering, School of Engineering, University of Alabama at Birmingham, Birmingham, AL, USA

⁵Department of Pediatrics, Department of Pharmacology & Physiology, School of Medicine and Health Sciences: George Washington University, Washington DC, USA

Email addresses of co-authors:

Luther M. Swift	(lswift2@childrensnational.org)
Rafael Jaimes III	(rjaimes@childrensnational.org)
Damon McCullough	(dmcculloug@childrensnational.org)
Morgan Burke	(mtburke@childrensnational.org)
Marissa Reilly	(mreilly@childrensnational.org)
Takuya Maeda	(tmaeda@childrensnational.org)
Hanyu Zhang	(hz@uab.edu)
Nobuyuki Ishibashi	(nishibas@childrensnational.org)
Jack M. Rogers	(jrogers@uab.edu)

Corresponding author:

Nikki Gillum Posnack (nposnack@childrensnational.org)

KEYWORDS:

fluorescence, imaging, electrophysiology, heart, electrocardiogram, optical mapping, optocardiography

SUMMARY:

The objective of this study was to establish a method for investigating cardiac dynamics using a translational animal model. The described experimental approach incorporates dual-emission optocardiography in conjunction with an electrophysiological study to assess electrical activity in an isolated, intact porcine heart model.

ABSTRACT:

Small animal models are most commonly used in cardiovascular research due to the availability of genetically modified species and lower cost compared to larger animals. Yet, larger mammals

are better suited for translational research questions related to normal cardiac physiology, pathophysiology, and preclinical testing of therapeutic agents. To overcome the technical barriers associated with employing a larger animal model in cardiac research, we describe an approach to measure physiological parameters in an isolated, Langendorff-perfused piglet heart. This approach combines two powerful experimental tools to evaluate the state of the heart: electrophysiology (EP) study and simultaneous optical mapping of transmembrane voltage and intracellular calcium using parameter sensitive dyes (RH237, Rhod2-AM). The described methodologies are well suited for translational studies investigating the cardiac conduction system, alterations in action potential morphology, calcium handling, excitation-contraction coupling and the incidence of cardiac alternans or arrhythmias.

INTRODUCTION:

Cardiovascular disease is a leading cause of illness and death worldwide. As such, a primary research focus is to optimize methodologies that can be used to study normal cardiac physiology and underlying mechanisms that can contribute to morbidity and mortality in humans. Basic cardiovascular research has traditionally relied on small animal models, including rodents and rabbits¹⁻³, due to the availability of genetically modified species^{4,5}, lower-cost, smaller experimental footprint, and higher throughput. However, the use of a pig model has the potential to provide more clinically relevant data⁶. Indeed, previous studies have documented similarities in cardiac electrophysiology (EP) between humans and pigs, including similar ion currents⁷, action potential shape⁸, and responses to pharmacological testing⁹. Moreover, the porcine heart has contractile and relaxation kinetics that are more comparable to humans than either rodents or rabbits¹⁰. Compared to a canine model, the porcine coronary anatomy more closely resembles a human heart^{11,12} and is the model of choice for studies focused on heart development, pediatric cardiology and/or congenital heart defects¹³. Although there are differences between the pig and human heart⁸, these similarities make the porcine heart a valuable model for cardiovascular research¹⁴.

Retrograde perfusion of the heart has become a standard protocol for studying cardiac dynamics ex vivo¹⁵ since first established by Oskar Langendorff¹⁶. Accordingly, Langendorff-perfusion can be used to support an isolated, intact heart in the absence of autonomic influences. This model is a useful tool for directly comparing cardiac electrophysiology and contractility between healthy and non-healthy hearts. Since cardiac dynamics are both temporally and spatially complex, a slight alteration in one region can dramatically affect the entire heart's ability to work as a syncytium¹⁷. Therefore, high spatiotemporal imaging of parameter sensitive dyes is a useful tool for monitoring cardiac function across the surface of the heart^{18,19}. Indeed, simultaneous dual imaging of voltage and calcium-sensitive fluorescent probes allows for the assessment of electrical activity, calcium handling and excitation-contraction coupling at the tissue level²⁰⁻²⁸. Langendorff-perfusion and/or optical mapping techniques have previously been used to document the decline in cardiac performance due to aging or genetic mutations, and to assess the safety of pharmacological agents or environmental exposures²⁹⁻³³.

In the clinical setting, an invasive cardiac electrophysiology study is often used to investigate cardiac rhythm disturbances, identify pathologies, and pinpoint possible treatment options.

Similarly, we describe an EP protocol that can be used to assess sinus node function, measure atrioventricular conduction, and identify the refractoriness of myocardial tissue. The described EP study can be performed in conjunction with optical mapping, or optocardiography³⁴, to fully characterize cardiac physiology in isolated hearts. In the described protocol, high spatiotemporal resolution fluorescence imaging was performed with a combination of voltage (RH237) and calcium (Rhod-2AM) dyes in a dual emission setup. Additionally, cardiac electrophysiology parameters were monitored under both sinus rhythm and in response to programmed electrical stimulation.

PROTOCOL:

All experiments were conducted in accordance with the National Institutes of Health Guide for the Care and Use of Laboratory Animals (Eighth Edition). All methods and protocols used in these studies have been approved by The Children's National Medical Center Institutional Animal Care and Use Protocol Committee following the Guidelines for Care and Use of Laboratory Animals published by NIH. All animals used in this study received humane care in compliance with the Guide for the Care and Use of Laboratory Animals.

1. Preparation

1.1. Prepare 6 L of modified Krebs-Henseleit solution¹⁶ (mM: 118.0 NaCl, 3.3 KCl, 1.2 MgSO₄, 24.0 NaHCO₃, 1.2 KH₂PO₄, 10.0 glucose, 2.0 sodium pyruvate, 2% albumin, 2.0 CaCl₂). Add CaCl₂ on the day of the experiment, since over time, in the presence of phosphates, calcium chloride will terminally precipitate out of solution as calcium phosphate.

1.2. Adjust the pH to 7.4 after sterile filtering (pore size: 0.22 µm). Check the solution osmolality to ensure a range of 275–310 mOsm/kg. Cool 1 L on ice for use immediately after the heart is excised. Warm 3 L in a water bath to approximately 37 °C before bubbling with carbogen (95% O₂, 5% CO₂).

NOTE: Warming minimizes bubbles and potential embolism, since cold liquid has an increased capacity of gas to dissolve; therefore, as the modified Krebs-Henseleit media passes through the perfusion system and warms, the gas will be released as bubbles.

1.3. Prepare 2 L of cardioplegia (modified del Nido cardioplegia solution, **Table 1**). Freeze enough cardioplegia in an ice cube tray to fill a 500 mL beaker.

1.4. Turn on the circulating water baths set to 42 °C. Turn on the pumps to circulate the perfusate in a closed hydronic heating loop (for a full list of materials, see **Table of Materials** and **Figure 1**).

NOTE: A heated circulating water bath is used to warm the water-jacketed tubes and heat exchangers.

1.5. Clean tubing circuits and chambers by running 2 L of a 1% solution of universal detergent in water through the system. Rinse all tubing circuits and chambers of the Langendorff system with >4 L of purified water. Run pumps until all water has been removed from the system.

1.6. Add a synthetic membrane filter in line with the perfusion pumps (polypropylene filter, pore size >5 µm). Gas a microfiber oxygenator (hemofilter) with 95% O₂ and 5% CO₂ at 80 kPa.

NOTE: When using albumin, there is often frothing associated with oxygenation and/or the pumping activity through the tubing circuit. An anti-foam compound (antifoam Y30 emulsion) can be added dropwise periodically (~every 30 min) to quench it as it occurs.

1.7. Check a two-point calibration (0 and 60 mmHg) for the pressure sensor located above the aorta or in the bubble trap; calibrate as needed.

1.8. Immediately before heart excision, pour the media into the Langendorff loop perfusion system. Ensure that perfusate passes through microfiber oxygenators (hemofilters) gassed with oxygenated perfusate, which then flows through heat exchangers to maintain a media perfusate temperature of 37 °C at the aorta.

1.9. Set the circulating water bath to a few degrees higher than 37 °C, such as 42 °C, to account for heat loss during exchange and throughout the system. Monitor the circulating perfusate temperature with thermocouples.

2. Heart excision and Langendorff-perfusion

2.1. Sedate the pig with an intramuscular (I.M.) injection of ketamine (20 mg/kg) and xylazine (2 mg/kg) and intubate with an endotracheal tube. For induction, administer an intravenous (I.V.) bolus injection of fentanyl (50 µg/kg) and rocuronium (1 mg/kg). Maintain anesthesia with inhaled Isoflurane (0.5–3%), fentanyl (10–25 µg/kg), and pancuronium (1 mg/kg).

NOTE: For this proof-of-principle study, juvenile Yorkshire pigs (14–42 days old, n = 18) were used that ranged from 2.5–10.5 kg body weight and 18–137 g heart weight (**Figure 2**). If an additional injection for induction is necessary, ketamine (10 mg/kg) can be injected I.M.

2.2. Once the animal is completely anesthetized and non-responsive, perform a sternotomy to expose the ascending aorta and right atrium.

2.2.1. Using a scalpel, make a midline incision from the top of the sternum at the thoracic inlet, down to the xiphoid process. With a cautery (or scissors), dissect the underlying fat and muscle until the sternum is visible.

2.2.2. From the xiphoid process, cut the sternum midline up through the manubrium with either surgical bone scissors or a bone saw. Insert retractors into the incision to expose the heart.

2.3. Deliver a bolus dose of heparin (300 units/kg) to the right atria, using an 18 G needle and syringe, to minimize blot clots upon organ excision. Place absorbent pads in the chest cavity and ice around the heart.

2.4. With scissors, carefully slice through the pericardium, isolate the aorta by blunt dissection from the surrounding connective tissue, and clamp the aorta just below the first arterial branch on the aortic arch. Using a 50 mL syringe with an 18 G needle, inject ice-cold cardioplegia (20 mL/kg) through the top of the ascending aorta.

2.5. Cut through the vessels leading to the heart and remove the heart with the ascending aorta intact and plunge the excised heart into ice-cold cardioplegia.

2.6. Grasp the walls of the aorta with a pair of hemostats and slip it onto a ribbed cannula attached to tubing leading to 1 L of ice cold cardioplegia media suspended above the heart (~95 cm to provide ~70 mm Hg). Allow fluid to enter and fill the aorta until it overflows to prevent any bubble from entering the vasculature.

NOTE: Use of a mechanical uncoupler (2,3-butanedione monoxime [BDM] or blebbistatin) will decrease the coronary perfusion rate as the oxygen demand of the tissue declines.

2.7. Secure the aorta to the cannula using umbilical tape and further anchor it by tying up the hemostats to bear the weight of the heart, which is now hanging from the cannula (**Figure 1C**). Allow the cold media to retrograde perfuse the heart at a constant pressure of 70 mmHg via gravity. Keep the heart submerged in cold cardioplegia until ready to be transferred to the warmed (37 °C) Langendorff-perfusion system (<10 min).

NOTE: The aorta on smaller hearts (<50 g, up to 2-week-old pig) will bear the weight of the heart but larger hearts are at risk of slipping off the cannula. During the initial cannulation and when moving to the warmed system, prevent air from entering the aorta, which can cause coronary emboli. Use large bore tubing (>3/8" internal diameter) which allows bubbles to rise faster than the solution entering the aorta.

2.8. Transfer the heart to the Langendorff system (37 °C) without introducing air into the cannula. Allow the normal sinus rhythm to flush the vasculature of any remaining blood and cardioplegia.

NOTE: In the described study an average initial flow rate of 184 ± 17 mL/min was observed in isolated juvenile piglet hearts. The flow rate declined to 70 ± 7.5 mL/min (mean \pm SEM) after perfusing with warmed media containing a mechanical uncoupler (20 mM BDM). Do not submerge the heart tissue, as it can impinge on cardiac imaging. Tissue temperature is maintained by coronary flow in the pig heart due to its larger volume and smaller surface area, as compared to rodents. Under full flow, the epicardium and endocardium temperatures ranged from 35 °C to 37 °C, respectively.

CAUTION: Wear appropriate personal protective equipment, including eye wear when working with mechanical uncouplers. The heart can eject media rapidly and unexpectedly.

2.9. Defibrillate the heart in the event of shockable arrhythmias (ventricular tachycardia, ventricular fibrillation) by placing external paddles at the apex and base of the heart and delivering a single shock at 5 J, increasing in 5 J increments (or as selectable by the defibrillator) until 50 J, cardioversion, or un-shockable rhythm. Repeat shocks at 50 J as necessary.

NOTE: In the presented study, 89% of preparations required defibrillation. After equilibration (~10 min), an average heart rate of 70 ± 4.5 bpm (mean \pm SEM) was observed for juvenile piglet hearts (**Figure 2**).

2.10. Flush the heart with at least 1 L of modified Krebs-Henseleit media, without recirculating, to remove any residual blood and cardioplegia. Once the media runs clear through the heart, close the circulating loop to recirculate perfusate.

3. Electrophysiology study

3.1. To record a standard lead II electrocardiogram (ECG) throughout the course of study, attach a 29 G needle electrode to the ventricular epicardium near the apex, with another electrode in the right atrium. Connect the positive and negative inputs of a differential bioamplifier to the apex and right atrium, respectively.

3.2. Attach one bipolar stimulus electrode on the right atria, and a second bipolar stimulus electrode to the lateral left ventricle for pacing purposes.

3.3. Pace the heart using an electrophysiology stimulator, with the initial current set to twice the diastolic threshold (1–2 mA) and a 1 ms pulse width^{35,36}.

NOTE: If the stimulation fails to elicit a response, the pulse width may be increased up to 2 ms. More current (~10x) is needed with large coaxial electrodes (bipolar stimulation).

3.4. Identify the pacing threshold by applying a series of stimulus impulses (1–2 mA, 1 ms pulse width) at defined pacing cycle lengths (PCL) to ensure consistent stimulus response.

NOTE: Once the intrinsic rate is established, the initial impulse train may begin at a slightly shorter PCL.

3.5. Perform extrastimulus pacing using either an S1–S1 or S1–S2 pacing train, in the latter a train of 6–8 impulses (S1) was followed by a single impulse (S2). Decrease the S2 PCL stepwise by 10 ms (i.e., 200 ms, 190 ms, 180 ms, etc.) until it fails to capture. Step up to the penultimate PCL (i.e., 190 ms) and decrease in 1 ms intervals to find the most precise PCL before the loss of capture (i.e., 184 ms).

NOTE: The same stimulation parameters are used for both S1 and S2 (1–2 mA, 1 ms pulse width). See **Figure 3** for representative examples, or previously published values on porcine heart electrophysiology measurements³⁷.

3.5.1. To establish the ventricular effective refractory period (VERP), use the stimulus electrode on the lateral left ventricle to identify the shortest S1–S2 interval at which the S2 (premature beat) initiates ventricular depolarization.

NOTE: The refractory period is the shortest achievable S1–S2 coupling interval.

3.5.2. To define the Wenckebach cycle length (WBCL), use the stimulus electrode on the right atrium to find the shortest S1–S1 interval at which 1:1 atrioventricular conduction propagates via the normal conduction pathway.

NOTE: Failure to do so represents 2nd degree heart block.

3.5.3. To define the sinus node recovery time (SNRT), use the stimulus electrode on the right atrium to apply a pacing train (S1–S1) and measure the time delay between the last impulse in the pacing train, and the recovery of spontaneous sinoatrial node-mediated activity.

3.5.4. To establish atrioventricular node effective refractory period (AVNERP), use the stimulus electrode on the right atrium to find the shortest S1–S2 coupling interval at which the premature atrial stimulation is followed by a His bundle potential that elicits a QRS complex, which signifies ventricular depolarization.

4. Optical mapping of transmembrane voltage and intracellular calcium

NOTE: A mechanical uncoupler should be used to minimize motion artifacts during optical mapping and to avoid hypoxia^{3, 38–40}. (–/–)Blebbistatin (5 μ M circulating concentration) may be added slowly as a bolus dose of 0.5 mM in 5 mL of perfusate (100x of final concentration)⁴¹. Alternatively, BDM may be initially included in the perfusate media at a circulating concentration of 20 mM.

4.1. Prepare the voltage dye by dissolving 5 mg of RH237 into 4 mL of anhydrous DMSO. Dilute the dye aliquot with up to 5 mL of media and vortex. Slowly add RH237 (62.1 μ g per 500 mL of perfusate) proximal to the aortic cannula.

NOTE: The myocardial tissue may be re-stained with RH237, if needed, throughout the duration of the experiment.

4.2. Prepare the calcium dye by dissolving 1 mg of Rhod2-AM into 1 mL of anhydrous DMSO. Mix the dye with 50 μ L of pluronic acid, place in a 37 °C sonicating bath for up to 10 min, and then dilute with up to 5 mL of media. Slowly add the calcium dye (50 μ g per 500 mL of perfusate) proximal to the aortic cannula.

NOTE: To ensure uniform dye staining, dyes should be added slowly (>30 s). Rhod-2AM takes up to 10 min to reach peak fluorescence, while RH237 stains the heart within a 1–2 min. Using the described dye loading, signal to noise ratio (SNR) ranges of ~42–86 and ~35–69 for voltage and calcium, respectively, can be expected. SNR values can be calculated as $SNR = (\text{Peak-to-Peak counts})/(\text{Standard deviation during diastolic interval})^{42}$.

4.3. Position the imaging hardware (camera, image splitter, lens) as shown in **Figure 1**, to focus on an appropriate field of view.

NOTE: The splitter is configured with a dichroic mirror (660+ nm) that passes RH237 and reflects Rhod2 emission spectra. High-transmission emission filters are used for the RH237 (710 nm long pass) and Rhod2 (585 ± 40 nm) emitted light (long pass ET710, see **Table of Materials**). A wide-pupil 50 mm/F0.95I lens is attached to the front of the image splitter. This configuration results in adequate emission light separation, as previously validated^{43, 44}.

4.4. Connect the camera to a workstation and acquire images using selected software, with an exposure time of 0.5–2 ms. Perform image alignment with the aid of software that can split the desired regions, overlay, and display a gray-scale subtraction or pseudo-color addition to highlight misalignment (see **Table of Materials** for software option).

4.5. Turn off the room light to minimize fluorescence interference from ambient lighting. Test the LED lights (525 nm, 1.4 mW/mm²) prior to the start of imaging to ensure uniform and maximal epicardial illumination, as determined by the sensor well depth.

NOTE: Each light is directed through an excitation filter (535 ± 25 nm). LED lights can be triggered manually before filming to maximize signal linearity. Emitted fluorescence from the epicardium is passed through the image splitter and emission filters. Split images are projected onto a high-speed sensor. The field of view of is approximately 12 cm x 10 cm, or 5.9 cm x 4.7 cm for each split image, depending on lens choice and distance from the heart.

4.6. For optical mapping studies, image the myocardium during sinus rhythm, ventricular fibrillation (**Figure 4**) or dynamic pacing (S1–S1, 1–2 mA, 1 ms pulse width) via a stimulation electrode positioned on the left ventricle (**Figure 5**). Begin with a pacing cycle length of 350 ms, and decrement by 10–50 ms to generate restitution curves (**Figure 5E**)^{35,36}.

5. Cleanup

5.1. Remove the heart from the system and drain all perfusate. Rinse the system tubing and chambers with purified water.

5.2. For routine maintenance, periodically rinse the system with detergent solution or a diluted hydrogen peroxide solution, as needed.

6. Data processing

6.1. Confirm optical signal quality throughout the study by opening a video file, selecting a region of interest, and plotting mean fluorescence over time using an appropriate software package or custom algorithm.

6.2. Analyze imaging data as previously described^{23,33,43,45,46}, to quantify action potential and calcium transient temporal parameters, including activation time, voltage-calcium coupling time (difference between Vm and Ca activation times), and repolarization duration measurements.

6.2.1. Apply thresholding to isolate fluorescent epicardial pixels and discard noisy background data.

NOTE: Thresholding will simplify and speed up analysis across large videos.

6.2.2. Spatially filter optical signals over an epicardial surface area with kernel sizes ranging from 3 mm x 3 mm to 5 mm x 5 mm, as seen in **Figure 4** and **Figure 5**.

NOTE: The latter will improve the SNR without distorting action potential features, calcium transient morphology, or overall contour of the wavefronts^{19,47}. This may be unnecessary if using a sensor with large pixels or if binning during acquisition.

6.2.3. Temporally filter signals with a digital lowpass filter (e.g., 5th-order Butterworth) with a cutoff frequency between 100 and 75 Hz to eliminate insignificant signal content⁴⁵.

NOTE: See **Figure 5C** for an example of representative processed traces.

6.2.4. Apply drift removal and subtraction, via Nth-order polynomial fitting, to minimize the effects of photobleaching, motion, or other significant sources of variation.

6.2.5. After processing and normalization of optical data across an entire video, calculate action potential and calcium transient parameters of interest. Determine activation time, defined as the time of maximum derivative during depolarization, and peak fluorescence in order to calculate repolarization percentage times and periods (action potential duration [APD] and [Ca²⁺]_i duration [CaD], see **Figure 5**).

6.2.6. After temporal parameters are calculated, generate isochronal maps to depict aspects of a single action potential or calcium transient across the entire imaged epicardial surface using custom algorithms^{23,33,43,45,46}.

NOTE: See **Figure 5D** for an example.

REPRESENTATIVE RESULTS:

Figure 1A shows a diagram of the isolated heart perfusion system, which includes the tubing circuit, pump, filter, oxygenator, reservoirs and heating elements. Placement of the ECG (lead II configuration) and pacing electrodes is shown in **Figure 1B**, and the imaging setup is depicted in **Figure 1C**. A schematic of the optical components and light paths are shown in **Figure 1D**.

Experimental studies were performed on intact, whole hearts isolated from juvenile Yorkshire pigs (14–42 days, $n = 18$) that ranged in size from 2.5–10.5 kg body weight and 18–137 g heart weight (**Figure 2A**). After transferring the isolated heart to a Langendorff system (37 °C), the heart rate stabilized to 70 ± 4.5 bpm (mean \pm SEM) within ~ 10 min of defibrillation and remained constant throughout the duration of study (**Figure 2B**). An average flow rate of 184 ± 17 mL/min (mean \pm SEM) was measured, which slowed to 70 ± 7.5 mL/min after perfusing with warmed media containing a mechanical uncoupler (**Figure 2C**).

Lead II ECGs were recorded throughout the duration of the study during sinus rhythm (**Figure 3A**) or in response to external pacing (**Figure 3B-E**) to quantify electrophysiological parameters. For EP assessment, dynamic pacing (S1–S1) was applied to the right atrium to pinpoint the WBCL and SNRT (recovery time after S1–S1 commences, **Figure 3C**), wherein WBCL was denoted as the shortest PCL that initiated atrial to ventricular conduction. An S1–S2 pacing protocol was implemented using a bipolar stimulus electrode on the left ventricle in order to identify the shortest coupling interval that initiated ventricular depolarization, thereby pinpointing VERP (**Figure 3D**). Alternatively, an S1–S2 atrial pacing protocol is applied to pinpoint AVNERP (S1–S2), as shown in **Figure 3E**. Representative examples of pig heart electrophysiology parameters align closely with those previously published³⁷.

Optical mapping experiments were performed during sinus rhythm, spontaneous ventricular fibrillation (**Figure 4**), or during dynamic pacing (S1–S1) of the left ventricle (LV) to generate electrical and calcium restitution curves depicted in **Figure 5**. Representative images of a dye-loaded piglet heart are shown in **Figure 4** with corresponding optical action potentials (V_m) and calcium (Ca) transients collected from two regions of interest on the epicardial surface (right ventricle [RV] = blue, LV = red). Unprocessed signals are displayed during sinus rhythm and during ventricular fibrillation. As previously mentioned, dynamic epicardial pacing (S1–S1) was also used during optical mapping experiments to normalize any slight difference in the intrinsic heart rate (**Figure 5A-E**). Raw signals are displayed (RV = blue, LV = red), which were used to depict the action potential – calcium transient coupling time (**Figure 5C**), activation and duration time (**Figure 5D**), electrical and calcium restitution (**Figure 5E**). For thick myocardial preparations, spatial filtering with kernel size ~ 3 mm \times 3 mm is appropriate for epicardial action potential or calcium transient analysis^{19, 47}. Accordingly, high spatial resolution images (in the described setup 1240 \times 1024 total, or 620 \times 512 per channel, 6.5 μ m pixel size) are often spatially binned during or post-acquisition (**Figure 5C**). Image processing can be performed to generate activation and repolarization maps using custom algorithms^{23, 33, 43, 45} (**Figure 3D**), with the activation time of each pixel on the heart was defined as the maximum derivative of the action potential or calcium transient upstroke.

FIGURE AND TABLE LEGENDS:

Figure 1: Experimental setup. (A) Diagram of the isolated heart perfusion system; arrows denote the direction of flow. (B) A cannulated heart is shown with electrode placement. RA = right atria, RV = right ventricle, LV = left ventricle, ECG = lead II electrocardiogram. (C) The imaging platform in close proximity to the heart tissue. (D) Emission of each complementary probe (voltage, calcium) is separated by wavelength using an image splitting device with appropriate emission filters and dichroic mirror.

Figure 2: Heart weight, rate and flow measurements. (A) Heart weight to body weight ratio for each piglet used in the study ($n = 18$). (B) Heart rate measured ~ 10 min after defibrillation and again at the end of study (approximately 1 h). (C) Coronary flow drops precipitously after perfusion with a mechanical uncoupler (+BDM) due to reduced oxygen demand. Scale bars represent mean \pm SEM.

Figure 3: Representative examples of lead II electrocardiogram recordings collected during sinus rhythm or in response to external pacing. (A) Normal sinus rhythm. (B) Example of epicardial pacing at cycle length of 400 ms (S1–S1), which was used for imaging experiments. (C) Top: Atrial pacing to identify WBCL; successful capture is observed at S1 = 250 ms wherein atrial to ventricular conduction is observed. Note that atrial pacing can be used to determine SNRT (time to sinus node discharge, after commencing external pacing). Bottom: As the S1 cycle length is decreased to 205 ms, the conduction to the ventricle fails. (D) Top: Epicardial pacing (S1–S2) to identify VERP; successful capture is observed at S1 = 450 ms, S2 = 300 ms. Bottom: As the S2 cycle length is decreased to 250 ms, the ventricular tissue fails to capture. (E) Atrial pacing (S1–S2) to identify AVNERP. Top: Successful capture is observed at S1 = 450 ms, S2 = 200 ms. Bottom: As the S2 cycle length is decreased to 199 ms, conduction to the ventricle fails. Blue arrows denote pacing spikes, red arrows denote capture ('C') or no capture ('NC'). S1–S1 = dynamic pacing, S1–S2 = extrastimulus pacing.

Figure 4: Optical data during sinus rhythm and ventricular fibrillation. Left: Representative images of a dye-loaded pig heart (Vm = voltage, RH237; Ca = calcium, Rhod2), anterior view. Center: Spatially filtered transmembrane voltage and intracellular calcium fluorescent signals from a pig heart during sinus rhythm. Right: Voltage and calcium signals during ventricular fibrillation. Signal region sizes (15 x 15 pixels = 2.4 x 2.4 mm, 30 x 30 = 4.8 x 4.8 mm kernel size) represented as red and blue squares. Units are $\Delta F/F$.

Figure 5: Optical data from Langendorff-perfused pig hearts. Unprocessed, spatially filtered (A) transmembrane voltage and (B) intracellular calcium fluorescence signals from the right and left ventricles during electrical pacing at the apex. Unfiltered, spatially averaged signals depict optical action potentials and calcium transients from regions of interest (signal units are $\Delta F/F$). (C) An overlay of normalized transients illustrates action potential-calcium transient coupling time (low-pass filtered at 75 Hz). (D) Processing signals across the epicardial surface to generate isochronal maps of temporal parameters, including activation time (t_{act}) and 80% repolarization time. (E) Electrical and calcium transient restitution curves generated at multiple frequencies (left) with

statistical analysis (right) to illustrate longer repolarization time at slower pacing cycle lengths. Scale bars represent mean \pm SEM.

Table 1: Modified del Nido's cardioplegia recipe.

DISCUSSION:

Although cardiovascular research models range from cellular to in vivo preparations, there is an inherent trade-off between clinical relevance and experimental utility. On this spectrum, the isolated Langendorff-perfused heart remains a useful compromise for studying cardiac physiology⁴⁸. The whole heart model represents a higher level of functional and structural integration than single cell or tissue monolayers, but also avoids the confounding complexities associated with in vivo models. A major advantage during dual optical mapping experiments is that the epicardial surface of the isolated heart can be observed, and fluorescence imaging of transmembrane potential and calcium handling can be used to monitor cardiac physiology³⁴.

Rodent models are most commonly used for isolated heart preparations as opposed to larger animals, due in part to the associated cost of up-sizing all the elements involved (e.g., solution volume, perfusion circuit, quantity of dyes and mechanical uncouplers) along with greater instability and propensity for arrhythmias in larger animals^{10,36,49}. One advantage to using pig hearts is that they closely resemble the human heart in structure, size and rate of contraction, therefore more accurately modeling hemodynamic parameters like coronary blood flow and cardiac output. Likewise, humans and pigs have similar calcium handling, electrocardiogram intervals³⁷, and action potential morphology including the underlying channels that it represents^{12,50–52}. This protocol describes in detail the steps for creating a reproducible large animal model to comprehensively characterize myocardial function. Simultaneous imaging of transmembrane voltage (RH237) and intracellular calcium (Rhod2), used in conjunction with established electrophysiological protocols, provides the opportunity to pinpoint mechanisms that are responsible for altered cardiac function. The described methodology can be used for preclinical safety testing, toxicological screening and the investigation of genetic or other disease pathologies. Moreover, the described methodology can be modified and adapted for use with other cardiac models (e.g., canine, human) depending on the specific research focus^{53–55}.

There are a few critical modifications to keep in mind when transitioning from a smaller rodent model to a larger pig model for isolated, whole heart preparations. During preparation and setup, we recommend adding albumin to the perfusate to maintain oncotic pressure and reduce edema (plus antifoam, if needed)^{56–59}. Moreover, perfusate containing albumin can also aid in metabolic studies that also require fatty acid-supplementation to the media^{60,61}. Unlike rodent hearts, the larger pig heart does not need to be submerged in warm media due to its smaller surface to volume ratio and the increased volume of warmed media flowing through the coronary vessels which better maintains the temperature. As noted earlier, we placed temperature probes inside the right ventricle and on the epicardial surface of both the right and left ventricles, observing only slight temperature fluctuations of 1–2 °C in all three locations throughout the study. Importantly, such faster flow rates can also increase the likelihood of bubbles and a potential embolism. To circumvent this problem, we recommend using a bubble trap with large bore

tubing leading straight down to the aortic cannula. Similarly, we found it most useful to have two individuals working in tandem to cannulate the aorta on a larger (and heavier) heart; one person to hold the aorta open with sturdy hemostats and another to secure the aorta to the cannula using umbilical tape. In the described methodology, we found that perfusion with cardioplegia and defibrillation were vital to cardiac recovery, which is contrary to rodent heart preparations. In our experience, only a few excised hearts resumed normal sinus-driven activity without cardioversion.

To improve optical imaging endpoints, a hanging heart preparation limited the effect of glare that can occur with a submerged heart. Moreover, the hanging heart also avoids any compression or compromise of the coronary vessels on the posterior aspect of the heart that can occur when laying the heart down horizontally for vertical imaging. We also found that loading fluorescent dyes after the bubble trap (close to the aortic cannula) greatly improved tissue staining and optical signals. Finally, to improve cardiac electrophysiology endpoints, the use of a larger coaxial stimulation electrode facilitated successful atrial pacing. Although we describe the use of electrocardiograms to identify capture and loss of capture for various EP parameters, intracardiac catheters or bipolar recording electrodes can also be used.

Our study was focused on developing a methodology for dual optical mapping and cardiac electrophysiological assessment in an isolated, intact porcine heart model. Due to similarities with the juvenile human heart, the porcine heart remains a popular model for studies focused on pediatric cardiology or congenital heart defects. Importantly, the described approach can be adapted to use with larger sized adult hearts and/or different species of interest. Indeed, other laboratories may find that the use of canine or human hearts (either donor or diseased) are more applicable for their specific research focus^{53–55}. Another potential limitation to this study is the use of a mechanical uncoupler to reduce motion artifact during imaging. Blebbistatin has become the uncoupler of choice in cardiac imaging applications due to its minimal effects on ECG parameters, activation and refractory periods^{41,62,63}. BDM is a less expensive choice, which can be particularly important in large animal studies that require greater volumes of perfusate and mechanical uncoupler, but it is known to have a greater impact on potassium and calcium currents that can alter action potential morphology^{64–67}. If BDM is used, note that APD shortening increases the heart's vulnerability to shock-induced arrhythmias⁶⁸. Conversely, the main limitation to using blebbistatin is its photosensitivity and phototoxicity, although alternative formulations that have reduced these effects^{69–71}. Finally, the described methodology utilizes a single camera system for dual optical mapping experimentation, but it is important to note that research studies focused on ventricular fibrillation and/or tracking of electrical waves across the epicardial surface would need to modify this approach to include three-dimensional panoramic imaging, as described by others^{15,19,72–75}.

ACKNOWLEDGMENTS:

The authors gratefully acknowledge Dr. Matthew Kay for helpful experimental guidance, and Manelle Ramadan and Muhaymin Chowdhury for technical assistance. This work was supported by the National Institutes of Health (R01HL139472 to NGP, R01 HL139712 to NI), Children's

Research Institute, Children's National Heart Institute and Sheikh Zayed Institute for Pediatric Surgical Innovation.

DISCLOSURES:

The authors have nothing to disclose.

REFERENCES:

1. Wang, L., De Jesus, N.M., Ripplinger, C.M. Optical Mapping of Intra-Sarcoplasmic Reticulum Ca^{2+} and Transmembrane Potential in the Langendorff-perfused Rabbit Heart. *Journal of Visualized Experiments*. (103), e53166 (2015).
2. Lang, D., Sulkin, M., Lou, Q., Efimov, I.R. Optical Mapping of Action Potentials and Calcium Transients in the Mouse Heart. *Journal of Visualized Experiments*. (55), e3275 (2012).
3. Asfour, H., Wengrowski, A.M., Jaimes III, R., Swift, L.M., Kay, M.W. NADH fluorescence imaging of isolated biventricular working rabbit hearts. *Journal of Visualized Experiments*. (65), e4115 (2012).
4. Capecchi, M.R. The new mouse genetics: altering the genome by gene targeting. *Trends in genetic*. **5** (3), 70–6 (1989).
5. Hall, B., Limaye, A., Kulkarni, A.B. Overview: generation of gene knockout mice. *Current Protocols in Cell Biology*. **Chapter 19**, Unit 19.12 19.12.1-17 (2009).
6. Schechter, M.A. *et al.* An Isolated Working Heart System for Large Animal Models. *Journal of Visualized Experiments*. (88), e51671 (2014).
7. Arlock, P. *et al.* Ion currents of cardiomyocytes in different regions of the Göttingen minipig heart. *Journal of Pharmacological and Toxicological Methods*. **86**, 12–18 (2017).
8. Crick, S.J., Sheppard, M.N., Ho, S.Y., Gebstein, L., Anderson, R.H. Anatomy of the pig heart: comparisons with normal human cardiac structure. *Journal of anatomy*. **193** (Pt 1) 105–19 (1998).
9. Markert, M. *et al.* Validation of the normal, freely moving Göttingen minipig for pharmacological safety testing. *Journal of Pharmacological and Toxicological Methods*. **60** (1), 79–87 (2009).
10. Milani-Nejad, N., Janssen, P.M.L.M.L. Small and large animal models in cardiac contraction research: advantages and disadvantages. *Pharmacology & Therapeutics*. **141** (3), 235–49 (2014).
11. Bertho, E., Gagnon, G. A comparative study in three dimension of the blood supply of the normal interventricular septum in human, canine, bovine, porcine, ovine and equine heart. *Diseases of the Chest*. **46**, 251–62 (1964).
12. Lelovas, P.P., Kostomitsopoulos, N.G., Xanthos, T.T. A comparative anatomic and physiologic overview of the porcine heart. *Journal of the American Association for Laboratory Animal Science*. **53** (5), 432–8 (2014).
13. Camacho, P., Fan, H., Liu, Z., He, J.-Q. Large Mammalian Animal Models of Heart Disease. *Journal of Cardiovascular Development and Disease*. **3** (4), 30 (2016).
14. Jordan, C.P. *et al.* Minimally Invasive Resynchronization Pacemaker: A Pediatric Animal Model. *The Annals of Thoracic Surgery*. **96** (6), 2210–2213 (2013).
15. Rogers, J.M., Walcott, G.P., Gladden, J.D., Melnick, S.B., Kay, M.W. Panoramic optical mapping reveals continuous epicardial reentry during ventricular fibrillation in the isolated swine heart. *Biophysical Journal*. **92** (3), 1090–1095 (2007).
16. Langendorff, O. Untersuchungen am überlebenden Säugethierherzen [Investigations on the

surviving mammalian heart]. *Pflügers Archiv: European Journal of Physiology*. **61**, 291–332 (1895).

17. Pumir, A., Arutunyan, A., Krinsky, V., Sarvazyan, N. Genesis of ectopic waves: role of coupling, automaticity, and heterogeneity. *Biophysical Journal*. **89** (4), 2332–2349 (2005).

18. Kay, M.W., Walcott, G.P., Gladden, J.D., Melnick, S.B., Rogers, J.M. Lifetimes of epicardial rotors in panoramic optical maps of fibrillating swine ventricles. *American journal of Physiology - Heart and Circulatory Physiology*. **291** (4), H1935–41 (2006).

19. Lee, P. et al. Low-Cost Optical Mapping Systems for Panoramic Imaging of Complex Arrhythmias and Drug-Action in Translational Heart Models. *Scientific Reports*. **7**, 43217 (2017).

20. Venkataraman, R., Holcomb, M.R., Harder, R., Knollmann, B.C., Baudenbacher, F. Ratiometric imaging of calcium during ischemia-reperfusion injury in isolated mouse hearts using Fura-2. *BioMedical Engineering OnLine*. **11** (1), 39 (2012).

21. Efimov, I.R., Nikolski, V.P., Salama, G. Optical Imaging of the Heart. *Circulation Research*. **95** (1), 21–33 (2004).

22. Zimmermann, W.H. et al. Three-dimensional engineered heart tissue from neonatal rat cardiac myocytes. *Biotechnology and Bioengineering*. **68** (1), 106–114 (2000).

23. Jaimes, R. et al. A Technical Review of Optical Mapping of Intracellular Calcium within Myocardial Tissue. *American Journal of Physiology-Heart and Circulatory Physiology*. **310** (11), H1388–401 (2016)

24. Herron, T.J., Lee, P., Jalife, J. Optical imaging of voltage and calcium in cardiac cells & tissues. *Circulation Research*. **110** (4), 609–623 (2012).

25. Guatimosim, S., Guatimosim, C., Song, L.-S. Imaging Calcium Sparks in Cardiac Myocytes. *Methods in Molecular Biology (Clifton, N.J.)*. **689**, 205 (2011).

26. Hou, J.H., Kralj, J.M., Douglass, A.D., Engert, F., Cohen, A.E. Simultaneous mapping of membrane voltage and calcium in zebrafish heart in vivo reveals chamber-specific developmental transitions in ionic currents. *Frontiers in Physiology*. **5**, 344 (2014).

27. Thomas, K., Goudy, J., Henley, T., Bressan, M. Optical Electrophysiology in the Developing Heart. *Journal of Cardiovascular Development and Disease*. **5** (2), 28 (2018).

28. Nikolski, V., Efimov, I. Fluorescent imaging of a dual-pathway atrioventricular-nodal conduction system. *Circulation Research*. **88** (3), E23–30 (2001).

29. Posnack, N.G. et al. Bisphenol A Exposure and Cardiac Electrical Conduction in Excised Rat Hearts. *Environmental Health Perspectives*. **122** (4), 384–90 (2014).

30. Garrott, K. et al. KATP channel inhibition blunts electromechanical decline during hypoxia in left ventricular working rabbit hearts. *The Journal of Physiology*. **595** (12), 3799–3813 (2017).

31. Wang, Z. et al. Exposure to Secondhand Smoke and Arrhythmogenic Cardiac Alternans in a Mouse Model. *Environmental Health Perspectives*. **126** (12), 127001 (2018).

32. Francis Stuart, S.D. et al. Age-related changes in cardiac electrophysiology and calcium handling in response to sympathetic nerve stimulation. *The Journal of Physiology*. **596** (17), 3977–3991 (2018).

33. Jaimes, R. et al. Plasticizer Interaction With the Heart: Chemicals Used in Plastic Medical Devices Can Interfere With Cardiac Electrophysiology. *Circulation: Arrhythmia and Electrophysiology*. **12** (7), (2019).

34. Boukens, B.J., Efimov, I.R. A century of optocardiography. *IEEE reviews in Biomedical Engineering*. **7**, 115–125 (2014).

35. Li, N., Wehrens, X.H. Programmed Electrical Stimulation in Mice. *Journal of Visualized Experiments*. (39), e1730 (2010).

36. Dor-Haim, H., Berenfeld, O., Horowitz, M., Lotan, C., Swissa, M. Reduced Ventricular Arrhythmogeneity and Increased Electrical Complexity in Normal Exercised Rats. *PLoS ONE*. **8** (6), e66658 (2013).

37. Noszczyk-Nowak, A. *et al.* Normal Values for Heart Electrophysiology Parameters of Healthy Swine Determined on Electrophysiology Study. *Advances in Clinical and Experimental Medicine*. **25** (6), 1249–1254 (2016).

38. Wengrowski, A.M., Kuzmiak-Glancy, S., Jaimes, R., Kay, M.W. NADH changes during hypoxia, ischemia, and increased work differ between isolated heart preparations. *American Journal of Physiology-Heart and Circulatory Physiology*. **306** (4), H529-37 (2014).

39. Schramm, M., Klieber, H.G., Daut, J. The energy expenditure of actomyosin-ATPase, Ca(2+)-ATPase and Na⁺,K⁺-ATPase in guinea-pig cardiac ventricular muscle. *The Journal of Physiology*. **481** (Pt 3), 647–62 (1994).

40. Kuzmiak-Glancy, S. *et al.* Cardiac performance is limited by oxygen delivery to the mitochondria in the crystalloid-perfused working heart. *American Journal of Physiology- Heart and Circulatory Physiology*. **314** (4), H704–H715 (2018).

41. Fedorov, V. V *et al.* Application of blebbistatin as an excitation-contraction uncoupler for electrophysiologic study of rat and rabbit hearts. *Heart Rhythm*. **4**, (5), 619–626 (2007).

42. Evertson, D.W. *et al.* High-Resolution High-Speed Panoramic Cardiac Imaging System. *IEEE Transactions on Biomedical Engineering*. **55** (3), 1241–1243 (2008).

43. Jaimes, R. *et al.* Lights, Camera, Path Splitter: A New Approach for Truly Simultaneous Dual Optical Mapping of the Heart with a Single Camera. *bioRxiv*. 651380 (2019).

44. Choi, B.R., Salama, G. Simultaneous maps of optical action potentials and calcium transients in guinea-pig hearts: mechanisms underlying concordant alternans. *Journal of Physiology*. **529** 171–188 (2000).

45. Laughner, J.I., Ng, F.S., Sulkin, M.S., Arthur, R.M., Efimov, I.R. Processing and analysis of cardiac optical mapping data obtained with potentiometric dyes. *American Journal of Physiology-Heart and Circulatory Physiology*. **303** (7), H753-65 (2012).

46. O’Shea, C. *et al.* ElectroMap: High-throughput open-source software for analysis and mapping of cardiac electrophysiology. *Scientific Reports*. **9** (1), 1389, doi: 10.1038/s41598-018-38263-2 (2019).

47. Mironov, S.F., Vetter, F.J., Pertsov, A.M. Fluorescence imaging of cardiac propagation: spectral properties and filtering of optical action potentials. *American Journal of Physiology-Heart and Circulatory Physiology*. **291** (1), H327-335 (2006).

48. Skrzypiec-Spring, M., Grotthus, B., Szelag, A., Schulz, R. Isolated heart perfusion according to Langendorff---still viable in the new millennium. *Journal of Pharmacological and Toxicological Methods*. **55** (2), 113–126 (2007).

49. Nishida, K., Michael, G., Dobrev, D., Nattel, S. Animal models for atrial fibrillation: clinical insights and scientific opportunities. *Europace*. **12** (2), 160–172 (2010).

50. Verdouw, P.D., Van Den Doel, M.A., De Zeeuw, S., Duncker, D.J. Animal models in the study of myocardial ischaemia and ischaemic syndromes. *Cardiovascular Research*. **39** (1), 121-135 (1998).

51. Camacho, P., Fan, H., Liu, Z., He, J.-Q. Large Mammalian Animal Models of Heart Disease.

700 *Journal of Cardiovascular Development and Disease*. **3** (4), 30 (2016).

701 52. Swindle, M.M., Makin, A., Herron, A.J., Clubb, F.J., Frazier, K.S. Swine as Models in Biomedical
702 Research and Toxicology Testing. *Veterinary Pathology*. **49** (2), 344–356 (2012).

703 53. Aras, K.K., Faye, N.R., Cathey, B., Efimov, I.R. Critical Volume of Human Myocardium
704 Necessary to Maintain Ventricular Fibrillation. *Circulation: Arrhythmia and Electrophysiology*. **11**
705 (11), e006692 (2018).

706 54. Hill, A.J. *et al.* In Vitro Studies of Human Hearts. *The Annals of Thoracic Surgery*. **79** (1), 168–
707 177 (2005).

708 55. Fedorov, V. V *et al.* Structural and functional evidence for discrete exit pathways that connect
709 the canine sinoatrial node and atria. *Circulation Research*. **104** (7), 915–923 (2009).

710 56. Jacob, M. *et al.* Albumin Augmentation Improves Condition of Guinea Pig Hearts After 4 hr of
711 Cold Ischemia. *Transplantation*. **87** (7), 956–965 (2009).

712 57. Segel, L.D., Ensunsa, J.L. Albumin improves stability and longevity of perfluorochemical-
713 perfused hearts. *American Journal of Physiology-Heart and Circulatory Physiology*. **254** (6),
714 H1105–H1112 (1988).

715 58. Sutherland, F.J., Hearse, D.J. The isolated blood and perfusion fluid perfused heart.
716 *Pharmacological Research*. **41** (6), 613–627 (2000).

717 59. Werner, J.C., Whitman, V., Fripp, R.R., Schuler, H.G., Morgan, H.E. Carbohydrate metabolism
718 in isolated, working newborn pig heart. *American Journal of Physiology-Endocrinology and*
719 *Metabolism*. **241** (5), E364–E371 (1981).

720 60. Liao, R., Podesser, B.K., Lim, C.C. The continuing evolution of the Langendorff and ejecting
721 murine heart: new advances in cardiac phenotyping. *American Journal of Physiology-Heart and*
722 *Circulatory Physiology*. **303** (2), H156–H167 (2012).

723 61. Kates, R.E., Yee, Y.G., Hill, I. Effect of albumin on the electrophysiologic stability of isolated
724 perfused rabbit hearts. *Journal of Cardiovascular Pharmacology*. **13** (1), 168–72 (1989).

725 62. Lou, Q., Li, W., Efimov, I.R. The role of dynamic instability and wavelength in arrhythmia
726 maintenance as revealed by panoramic imaging with blebbistatin vs. 2,3-butanedione
727 monoxime. *American Journal of Physiology-Heart and Circulatory Physiology*. **302** (1), H262-9
728 (2012).

729 63. Swift, L.M., *et al.* Properties of blebbistatin for cardiac optical mapping and other imaging
730 applications. *Pflügers Archiv: European Journal of Physiology*. **464** (5), 503–512 (2012).

731 64. Kettlewell, S., Walker, N.L., Cobbe, S.M., Burton, F.L., Smith, G.L. The electrophysiological and
732 mechanical effects of 2,3-butane-dione monoxime and cytochalasin-D in the Langendorff
733 perfused rabbit heart. *Experimental Physiology*. **89** (2), 163–172 (2004).

734 65. Liu, Y. *et al.* Effects of diacetyl monoxime on the electrical properties of sheep and guinea pig
735 ventricular muscle. *Cardiovascular Research*. **27** (11), 1991–1997 (1993).

736 66. Jou, C.J., Spitzer, K.W., Tristani-Firouzi, M. Blebbistatin effectively uncouples the excitation-
737 contraction process in zebrafish embryonic heart. *Cellular Physiology and Biochemistry*. **25** (4–5),
738 419–24 (2010).

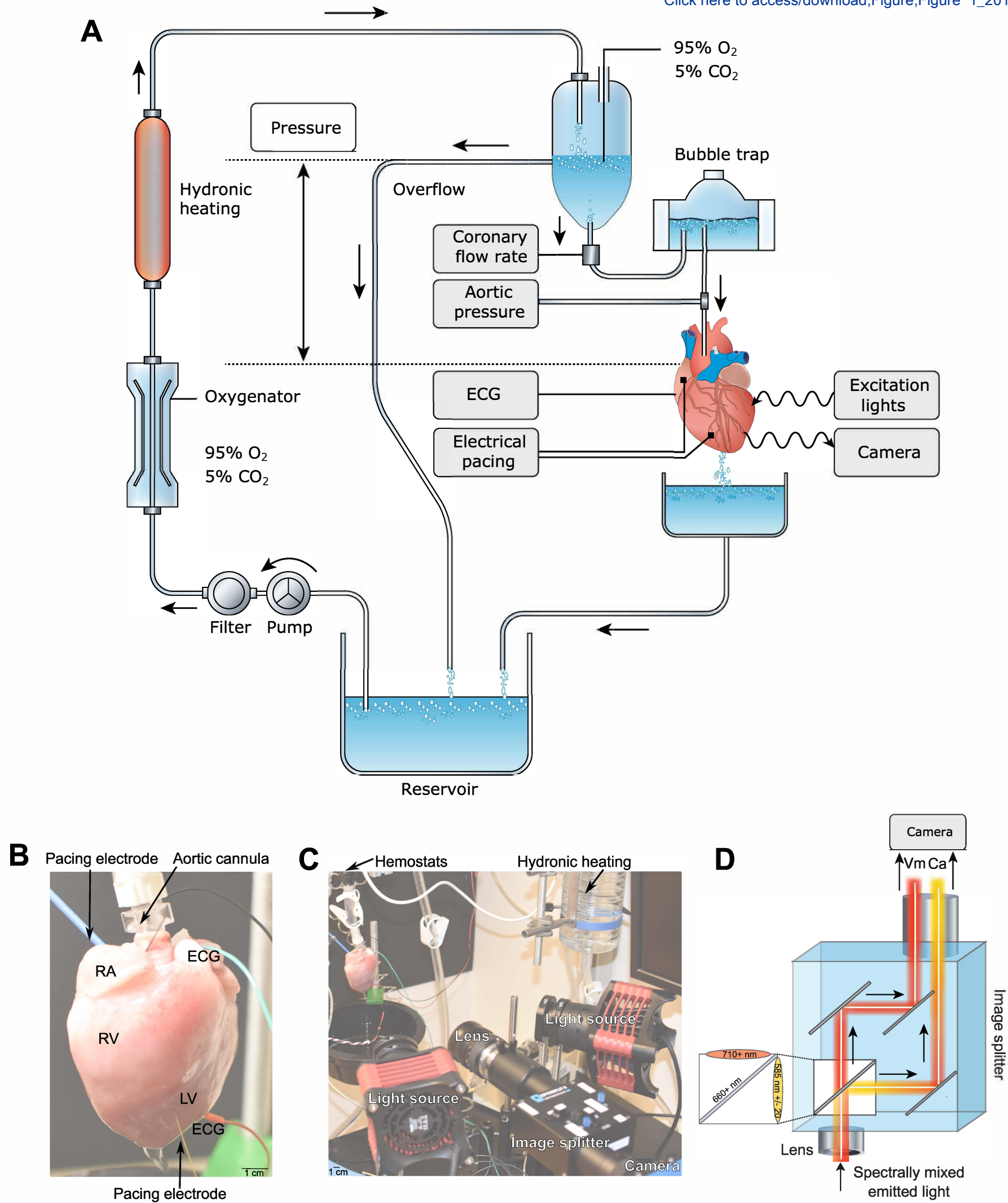
739 67. Sellin, L.C., McArdle, J.J. Multiple effects of 2,3-butanedione monoxime. *Pharmacology &*
740 *Toxicology*. **74** (6), 305–13 (1994).

741 68. Cheng, Y., Li, L., Nikolski, V., Wallick, D.W., Efimov, I.R. Shock-induced arrhythmogenesis is
742 enhanced by 2,3-butanedione monoxime compared with cytochalasin D. *American Journal of*
743 *Physiology-Heart and Circulatory Physiology*. **286** (1), H310–H318 (2004).

69. Kolega, J. Phototoxicity and photoinactivation of blebbistatin in UV and visible light. *Biochemical and Biophysical Research Communications*. **320** (3), 1020–1025 (2004).
70. Sakamoto, T., Limouze, J., Combs, C.A., Straight, A.F., Sellers, J.R. Blebbistatin, a myosin II inhibitor, is photoinactivated by blue light. *Biochemistry*. **44** (2), 584–588 (2005).
71. Várkuti, B.H. et al. A highly soluble, non-phototoxic, non-fluorescent blebbistatin derivative. *Scientific Reports*. **6** (1) 26141 (2016).
72. Bray, M.A., Lin, S.F., Wikswo Jr, J.P. Three-dimensional surface reconstruction and fluorescent visualization of cardiac activation. *IEEE Transactions on Bio-medical Engineering*. **47** (10), 1382–1391 (2000).
73. Qu, F., Ripplinger, C.M., Nikolski, V.P., Grimm, C., Efimov, I.R. Three-dimensional panoramic imaging of cardiac arrhythmias in rabbit heart. *Journal of Biomedical Optics*. **12** (4), 44019 (2007).
74. Gloschat, C. et al. RHYTHM: An Open Source Imaging Toolkit for Cardiac Panoramic Optical Mapping. *Scientific Reports*. **8** (1), 2921 (2018).
75. Kay, M.W., Amison, P.M., Rogers, J.M. Three-dimensional surface reconstruction and panoramic optical mapping of large hearts. *IEEE Transactions on Bio-medical Engineering*. **51** (7), 1219–1229 (2004).

Figure 1

[Click here to access/download;Figure;Figure 1_20190813_RE.pdf](#)



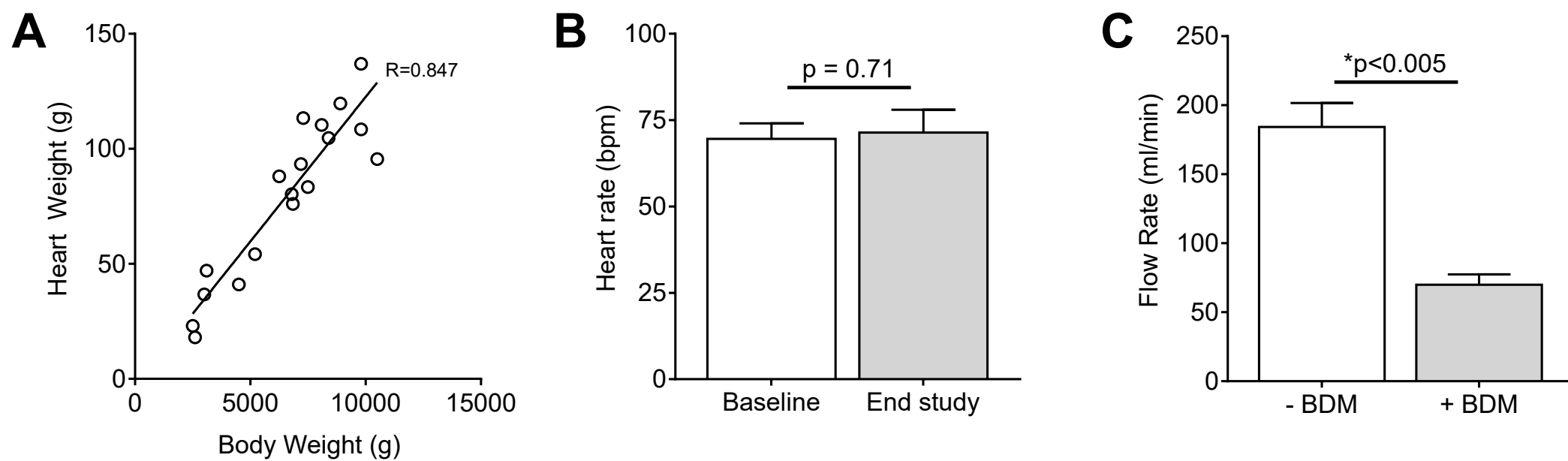
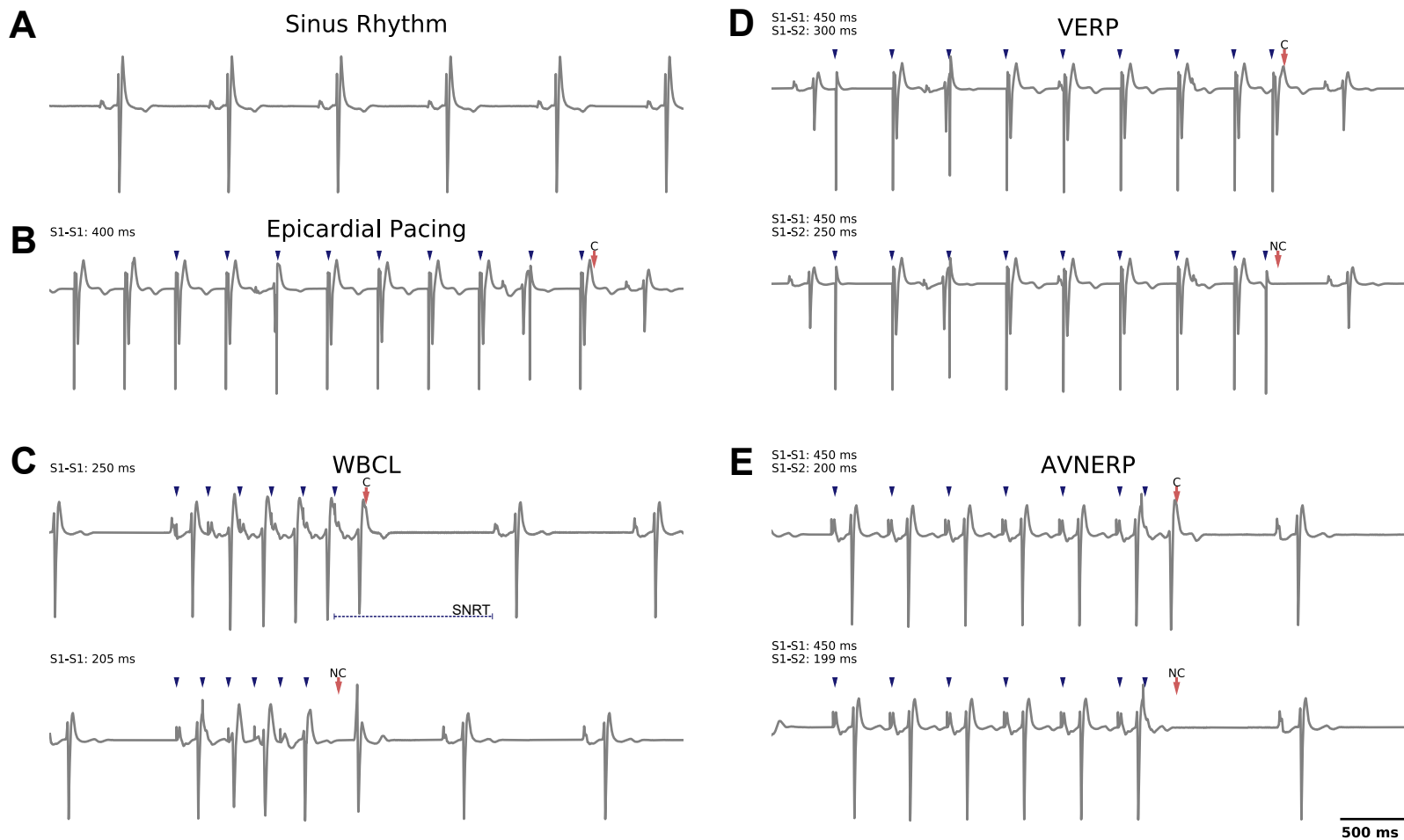


Figure 3

[Click here to access/download;Figure;Figure 3_20190813.pdf](#)



Sinus Rhythm [Click here to access/download;Figure;Figure 4_20190816.pdf](#) **Ventricular Fibrillation**

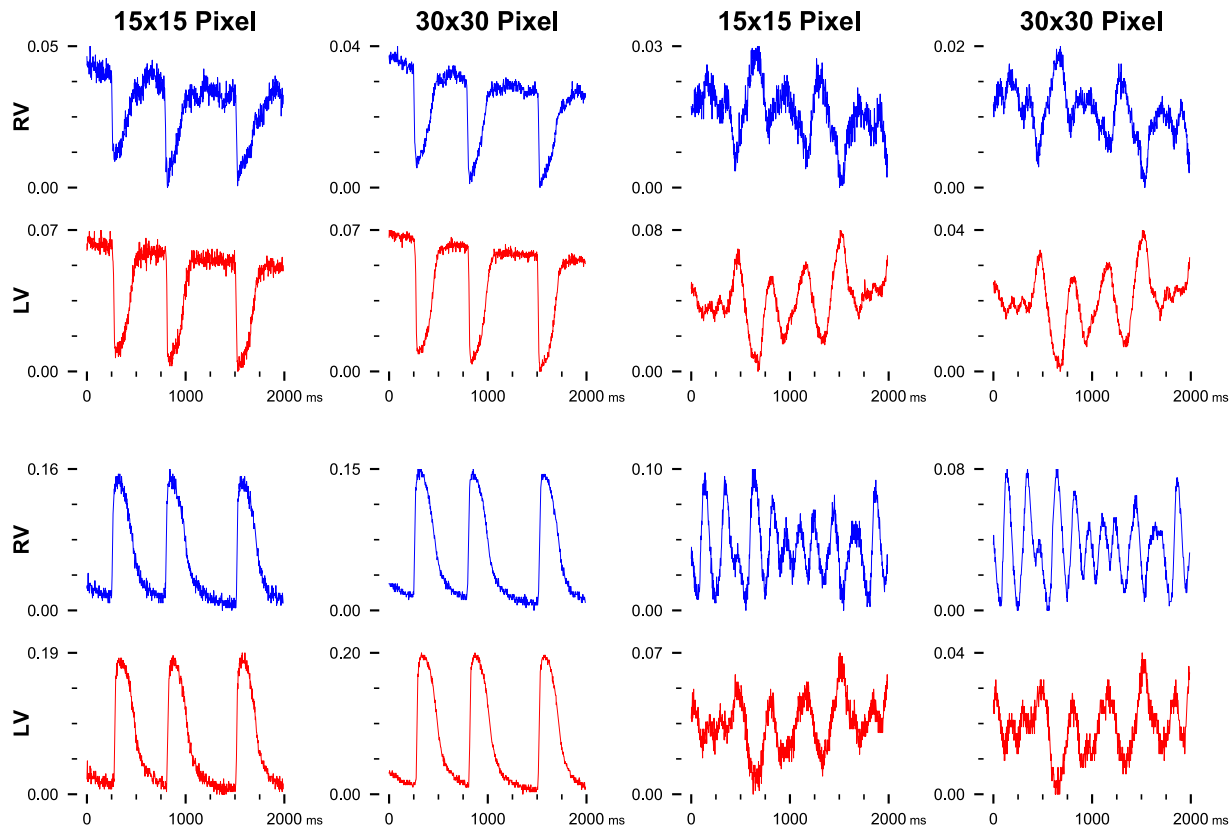
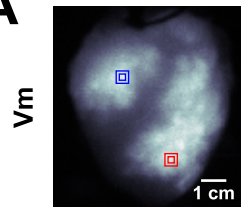
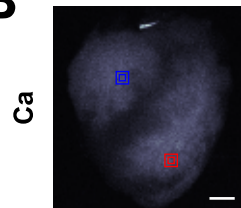


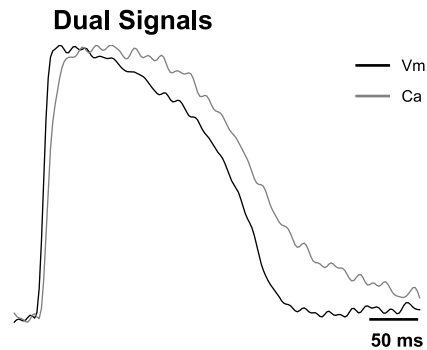
Figure 5
A Dual-Images



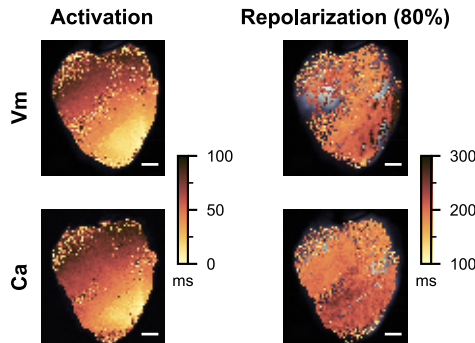
B



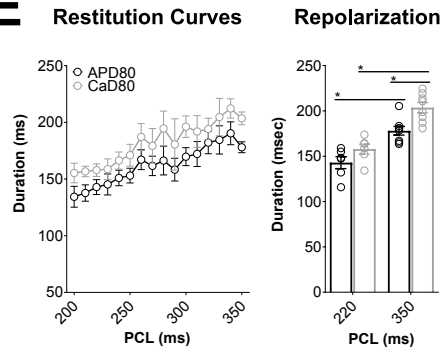
C



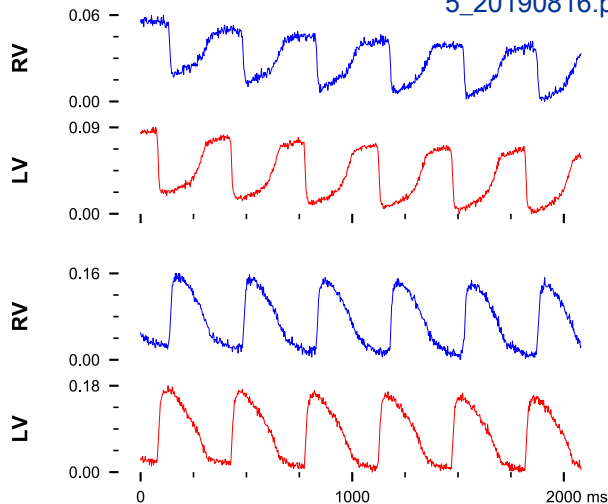
D



E

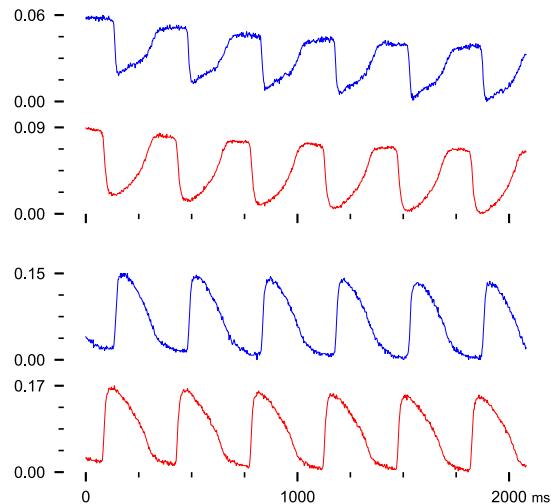


15x15 Pixel



Click here to access/download;Figure-Figure 5_20190816.pdf

30x30 Pixel



Chemical	Formula	Molecular weight	g/L	
Sodium chloride	NaCl	58.44	5.26	
Sodium gluconate	C ₆ H ₁₁ NaO ₇	218.14	5.02	
Sodium acetate trihydrate	C ₂ H ₃ NaO ₂ •3H ₂ O	136.08	3.68	
Potassium chloride	KCl	74.55	0.63	
Magnesium chloride (anhydrous)	MgCl ₂	95.21	0.1405	
8.4% Sodium bicarbonate	NaHCO ₃	84.01	13	
Mannitol	C ₆ H ₁₄ O ₆	182.17	16.3	
Magnesium sulfate	MgSO ₄	120.37	4	
pH	7.4			
Osmolarity (mOsmol/L)	294			

Name of Material/Equipment	Company	Catalog Number
(-)-Blebbistatin	Sigma-Aldrich	B0560-5MG
2,3-Butanedione monoxime (BDM)	Sigma-Aldrich	B0753-100G
Albumin	Sigma-Aldrich, St. Louis, MO	A9418
Analog signal interface	emka Technologies	itf16USB
Antifoam	Sigma-Aldrich	A5758-250ML
Antifoam Y-30 Emulsion	Sigma-Aldrich, St. Louis, MO	A5758
Aortic cannula, 5/16"	Cole-Parmer	45509-60
Bubble trap	Sigma-Aldrich	CLS430641U-100EA
CaCl ₂	Fisher Scientific, Fair Lawn, NJ	C77-500
Camera, sCMOS	Andor Technology	Zyla 4.2 PLUS
Coaxial stimulation electrode (atria)	Harvard Apparatus	73-0219
Defibrillator	Zoll	M Series
Dichroic mirror	Chroma Technology	T660lpxrxt-UF2
Differential amplifier	Warner Instruments	DP-304A
Emission filter, calcium	Chroma Technology	ET585/40m
Emission filter, voltage	Chroma Technology	ET710lp
EP stimulator (Bloom)	Fisher Medical	DTU-215B
Excitation filter	Chroma Technology	CT510/60bp
Excitation lights	Thorlabs	SOLIS-525C
Filter	McMaster-Carr	8147K52
Filter cartridge, polypropylene	Pentair	PD-5-934
Filter housing	McMaster-Carr	9979T21
Flow transducer	Transonic	ME6PXN
Glucose	Sigma-Aldrich, St. Louis, MO	158968
Heating coil	Radnoti	158821
Hemofilter	Hemocor	HPH 400
Hemostatic Forceps	World Precision Instruments	501326
Image Splitter	Cairn Research	OptoSplit II
KCl	Sigma-Aldrich, St. Louis, MO	P3911
KH ₂ PO ₄	Fisher Scientific, Fair Lawn, NJ	423-316
Large-bore tubing, I.D. 3/8"	Fisher Scientific	14-169-7H

Lens 50 mm, 0.95 f-stop	Navitar	DO-5095
Metamorph	Molecular Devices	
MgSO ₄	Sigma-Aldrich, St. Louis, MO	M-7506
Mucosal detergent	Sigma-Aldrich	Z637181-2L
Na Pyruvate	Sigma-Aldrich, St. Louis, MO	P2256
NaCl	Sigma-Aldrich, St. Louis, MO	S-3014
NaHCO ₃	Fisher Scientific, Fair Lawn, NJ	S-233
Needle Electrodes 29 gauge, 2 mm	AD Instruments Inc.	MLA1204
Noise eliminator	Quest Scientific	Humbug
Perfusion pump	PolyStan	A/S 1481
Pressure transducer	World Precision Instruments	BLPR2
Reservoir, 2 liter	Cole-Parmer	UX-34541-07
RH237	AAT Bioquest Inc.	21480
Rhod2-AM	AAT Bioquest Inc.	21062
Stimulation electrode (ventricle)	Harvard Apparatus	73-0160
Surgical Suture	McKesson Medical-Surgical	890186
Transducer amplifier	World Precision Instruments	TBM4M
Tubing flow console	Transonic	TS410
Umbilical tape	Jorvet	J0025UA
Water bath/circulator	VWR	89400-970

Surgical Tools

Bandage shears	Harvard Apparatus	72-8448
Electrocautery	Dalwha Corp. Ltd.	BA2ALD001
Hemostat	Roboz	RS-7476
Hemostatic forceps	Harvard Apparatus	72-8960
Hemostats	Harvard Apparatus	72-8985
Mayo scissors	WPI	501749
Metzenbaum scissors	WPI	501747
Mosquito forceps	Harvard Apparatus	72-8980
Needle holder	Harvard Apparatus	72-8828

Pediatric cross clamp	Roboz	RS-7660
Right angle forceps	WPI	501240
Scalpel	Ted Pella	549-4
scissors	Harvard Apparatus	72-8380
Straight Serrated forceps	WPI	500363
Towel clamp	WPI	501700
Weitlaner retractor	WPI	501314

Disposables

3-0 prolene suture	Various vendors	Various vendors
Vessel loop	Aspen surgical	011001PBX
Cardioplegia (Plegisol)	Pfizer	00409-7969-05
Heparin	Various vendors	Various vendors
Syringe and Needle	Various vendors	Various vendors
Umbilical tape	Ethicon	U12T

	Comments/Description
Mechanical Uncoupler	
Mechanical Uncoupler	

Image Alignment

Lister Bandage Scissors, Angled, Blunt/Blunt, 42.0mm blade length, 17.0 cm

Model: 200 Basic

St Vincent Tube Occluding Forceps

Hartmann Hemostatic Forceps, Curved, Serrated 2.2 mm tip width, 9.5 cm

Halstead-Mosquito Hemostatic Forceps Curved, Serrated, 2mm tip 14cm

14.5 cm, Straight

11.5 cm, Straight

Halstead-Mosquito Hemostatic Forceps Straight, Smooth, 2mm tip width 12cm

Webster Needle Holders, Straight, Smooth, 13.0 cm overall length

Cooley-Derra Clamp 6.25" 5mm Calibrations

Baby Mixer Hemostatic Forceps, 14cm, Right Angle

Scalpel Handle No. 4, 13.7cm Stainless Steel and 10 No. 22 Blades

Operating Scissors, Straight, Blunt/Blunt, 42mm blade, 12cm

Dressing Forceps 15.5cm

Backhaus Towel Clamp, 13cm, Curved, Locking handle, SS

Weitlaner Retractor, Self-Retaining, 10.2cm, 2x3 Sharp Prongs

Sterion® Vessel Loop, 0.8 x 406mm

Plegisol; St Thomas crystalloid cardioplegia solution 20ml/kg

300 U/kg

60mL & 18G respectively

ARTICLE AND VIDEO LICENSE AGREEMENT

Title of Article:	Optocardiography and Electrophysiology Studies of Ex Vivo Langendorff-perfused Pig Hearts
Author(s):	Swift, Jaimes, McCullough, Burke, Maeda, Zhang, Ishibashi, Rogers, Posnack

Item 1: The Author elects to have the Materials be made available (as described at <http://www.jove.com/publish>) via:

☐ Standard Access ☒ Open Access

Item 2: Please select one of the following items:

- ☒ The Author is **NOT** a United States government employee.
- ☐ The Author is a United States government employee and the Materials were prepared in the course of his or her duties as a United States government employee.
- ☐ The Author is a United States government employee but the Materials were NOT prepared in the course of his or her duties as a United States government employee.

ARTICLE AND VIDEO LICENSE AGREEMENT

1. **Defined Terms.** As used in this Article and Video License Agreement, the following terms shall have the following meanings: **"Agreement"** means this Article and Video License Agreement; **"Article"** means the article specified on the last page of this Agreement, including any associated materials such as texts, figures, tables, artwork, abstracts, or summaries contained therein; **"Author"** means the author who is a signatory to this Agreement; **"Collective Work"** means a work, such as a periodical issue, anthology or encyclopedia, in which the Materials in their entirety in unmodified form, along with a number of other contributions, constituting separate and independent works in themselves, are assembled into a collective whole; **"CRC License"** means the Creative Commons Attribution-Non Commercial-No Derivs 3.0 Unported Agreement, the terms and conditions of which can be found at: <http://creativecommons.org/licenses/by-nc-nd/3.0/legalcode>; **"Derivative Work"** means a work based upon the Materials or upon the Materials and other pre-existing works, such as a translation, musical arrangement, dramatization, fictionalization, motion picture version, sound recording, art reproduction, abridgment, condensation, or any other form in which the Materials may be recast, transformed, or adapted; **"Institution"** means the institution, listed on the last page of this Agreement, by which the Author was employed at the time of the creation of the Materials; **"JoVE"** means MyJoVE Corporation, a Massachusetts corporation and the publisher of The Journal of Visualized Experiments; **"Materials"** means the Article and / or the Video; **"Parties"** means the Author and JoVE; **"Video"** means any video(s) made by the Author, alone or in conjunction with any other parties, or by JoVE or its affiliates or agents, individually or in collaboration with the Author or any other parties, incorporating all or any portion

of the Article, and in which the Author may or may not appear.

2. **Background.** The Author, who is the author of the Article, in order to ensure the dissemination and protection of the Article, desires to have the JoVE publish the Article and create and transmit videos based on the Article. In furtherance of such goals, the Parties desire to memorialize in this Agreement the respective rights of each Party in and to the Article and the Video.

3. **Grant of Rights in Article.** In consideration of JoVE agreeing to publish the Article, the Author hereby grants to JoVE, subject to **Sections 4** and **7** below, the exclusive, royalty-free, perpetual (for the full term of copyright in the Article, including any extensions thereto) license (a) to publish, reproduce, distribute, display and store the Article in all forms, formats and media whether now known or hereafter developed (including without limitation in print, digital and electronic form) throughout the world, (b) to translate the Article into other languages, create adaptations, summaries or extracts of the Article or other Derivative Works (including, without limitation, the Video) or Collective Works based on all or any portion of the Article and exercise all of the rights set forth in (a) above in such translations, adaptations, summaries, extracts, Derivative Works or Collective Works and (c) to license others to do any or all of the above. The foregoing rights may be exercised in all media and formats, whether now known or hereafter devised, and include the right to make such modifications as are technically necessary to exercise the rights in other media and formats. If the "Open Access" box has been checked in **Item 1** above, JoVE and the Author hereby grant to the public all such rights in the Article as provided in, but subject to all limitations and requirements set forth in, the CRC License.

ARTICLE AND VIDEO LICENSE AGREEMENT

4. **Retention of Rights in Article.** Notwithstanding the exclusive license granted to JoVE in **Section 3** above, the Author shall, with respect to the Article, retain the non-exclusive right to use all or part of the Article for the non-commercial purpose of giving lectures, presentations or teaching classes, and to post a copy of the Article on the Institution's website or the Author's personal website, in each case provided that a link to the Article on the JoVE website is provided and notice of JoVE's copyright in the Article is included. All non-copyright intellectual property rights in and to the Article, such as patent rights, shall remain with the Author.

5. **Grant of Rights in Video – Standard Access.** This **Section 5** applies if the "Standard Access" box has been checked in **Item 1** above or if no box has been checked in **Item 1** above. In consideration of JoVE agreeing to produce, display or otherwise assist with the Video, the Author hereby acknowledges and agrees that, Subject to **Section 7** below, JoVE is and shall be the sole and exclusive owner of all rights of any nature, including, without limitation, all copyrights, in and to the Video. To the extent that, by law, the Author is deemed, now or at any time in the future, to have any rights of any nature in or to the Video, the Author hereby disclaims all such rights and transfers all such rights to JoVE.

6. **Grant of Rights in Video – Open Access.** This **Section 6** applies only if the "Open Access" box has been checked in **Item 1** above. In consideration of JoVE agreeing to produce, display or otherwise assist with the Video, the Author hereby grants to JoVE, subject to **Section 7** below, the exclusive, royalty-free, perpetual (for the full term of copyright in the Article, including any extensions thereto) license (a) to publish, reproduce, distribute, display and store the Video in all forms, formats and media whether now known or hereafter developed (including without limitation in print, digital and electronic form) throughout the world, (b) to translate the Video into other languages, create adaptations, summaries or extracts of the Video or other Derivative Works or Collective Works based on all or any portion of the Video and exercise all of the rights set forth in (a) above in such translations, adaptations, summaries, extracts, Derivative Works or Collective Works and (c) to license others to do any or all of the above. The foregoing rights may be exercised in all media and formats, whether now known or hereafter devised, and include the right to make such modifications as are technically necessary to exercise the rights in other media and formats. For any Video to which this **Section 6** is applicable, JoVE and the Author hereby grant to the public all such rights in the Video as provided in, but subject to all limitations and requirements set forth in, the CRC License.

7. **Government Employees.** If the Author is a United States government employee and the Article was prepared in the course of his or her duties as a United States government employee, as indicated in **Item 2** above, and any of the licenses or grants granted by the Author hereunder exceed the scope of the 17 U.S.C. 403, then the rights granted hereunder shall be limited to the maximum

rights permitted under such statute. In such case, all provisions contained herein that are not in conflict with such statute shall remain in full force and effect, and all provisions contained herein that do so conflict shall be deemed to be amended so as to provide to JoVE the maximum rights permissible within such statute.

8. **Protection of the Work.** The Author(s) authorize JoVE to take steps in the Author(s) name and on their behalf if JoVE believes some third party could be infringing or might infringe the copyright of either the Author's Article and/or Video.

9. **Likeness, Privacy, Personality.** The Author hereby grants JoVE the right to use the Author's name, voice, likeness, picture, photograph, image, biography and performance in any way, commercial or otherwise, in connection with the Materials and the sale, promotion and distribution thereof. The Author hereby waives any and all rights he or she may have, relating to his or her appearance in the Video or otherwise relating to the Materials, under all applicable privacy, likeness, personality or similar laws.

10. **Author Warranties.** The Author represents and warrants that the Article is original, that it has not been published, that the copyright interest is owned by the Author (or, if more than one author is listed at the beginning of this Agreement, by such authors collectively) and has not been assigned, licensed, or otherwise transferred to any other party. The Author represents and warrants that the author(s) listed at the top of this Agreement are the only authors of the Materials. If more than one author is listed at the top of this Agreement and if any such author has not entered into a separate Article and Video License Agreement with JoVE relating to the Materials, the Author represents and warrants that the Author has been authorized by each of the other such authors to execute this Agreement on his or her behalf and to bind him or her with respect to the terms of this Agreement as if each of them had been a party hereto as an Author. The Author warrants that the use, reproduction, distribution, public or private performance or display, and/or modification of all or any portion of the Materials does not and will not violate, infringe and/or misappropriate the patent, trademark, intellectual property or other rights of any third party. The Author represents and warrants that it has and will continue to comply with all government, institutional and other regulations, including, without limitation all institutional, laboratory, hospital, ethical, human and animal treatment, privacy, and all other rules, regulations, laws, procedures or guidelines, applicable to the Materials, and that all research involving human and animal subjects has been approved by the Author's relevant institutional review board.

11. **JoVE Discretion.** If the Author requests the assistance of JoVE in producing the Video in the Author's facility, the Author shall ensure that the presence of JoVE employees, agents or independent contractors is in accordance with the relevant regulations of the Author's institution. If more than one author is listed at the beginning of this Agreement, JoVE may, in its sole

ARTICLE AND VIDEO LICENSE AGREEMENT

discretion, elect not take any action with respect to the Article until such time as it has received complete, executed Article and Video License Agreements from each such author. JoVE reserves the right, in its absolute and sole discretion and without giving any reason therefore, to accept or decline any work submitted to JoVE. JoVE and its employees, agents and independent contractors shall have full, unfettered access to the facilities of the Author or of the Author's institution as necessary to make the Video, whether actually published or not. JoVE has sole discretion as to the method of making and publishing the Materials, including, without limitation, to all decisions regarding editing, lighting, filming, timing of publication, if any, length, quality, content and the like.

12. **Indemnification.** The Author agrees to indemnify JoVE and/or its successors and assigns from and against any and all claims, costs, and expenses, including attorney's fees, arising out of any breach of any warranty or other representations contained herein. The Author further agrees to indemnify and hold harmless JoVE from and against any and all claims, costs, and expenses, including attorney's fees, resulting from the breach by the Author of any representation or warranty contained herein or from allegations or instances of violation of intellectual property rights, damage to the Author's or the Author's institution's facilities, fraud, libel, defamation, research, equipment, experiments, property damage, personal injury, violations of institutional, laboratory, hospital, ethical, human and animal treatment, privacy or other rules, regulations, laws, procedures or guidelines, liabilities and other losses or damages related in any way to the submission of work to JoVE, making of videos by JoVE, or publication in JoVE or elsewhere by JoVE. The Author shall be responsible for, and shall hold JoVE harmless from, damages caused by lack of sterilization, lack of cleanliness or by contamination due to


the making of a video by JoVE its employees, agents or independent contractors. All sterilization, cleanliness or decontamination procedures shall be solely the responsibility of the Author and shall be undertaken at the Author's expense. All indemnifications provided herein shall include JoVE's attorney's fees and costs related to said losses or damages. Such indemnification and holding harmless shall include such losses or damages incurred by, or in connection with, acts or omissions of JoVE, its employees, agents or independent contractors.

13. **Fees.** To cover the cost incurred for publication, JoVE must receive payment before production and publication of the Materials. Payment is due in 21 days of invoice. Should the Materials not be published due to an editorial or production decision, these funds will be returned to the Author. Withdrawal by the Author of any submitted Materials after final peer review approval will result in a US\$1,200 fee to cover pre-production expenses incurred by JoVE. If payment is not received by the completion of filming, production and publication of the Materials will be suspended until payment is received.

14. **Transfer, Governing Law.** This Agreement may be assigned by JoVE and shall inure to the benefits of any of JoVE's successors and assignees. This Agreement shall be governed and construed by the internal laws of the Commonwealth of Massachusetts without giving effect to any conflict of law provision thereunder. This Agreement may be executed in counterparts, each of which shall be deemed an original, but all of which together shall be deemed to be one and the same agreement. A signed copy of this Agreement delivered by facsimile, e-mail or other means of electronic transmission shall be deemed to have the same legal effect as delivery of an original signed copy of this Agreement.

A signed copy of this document must be sent with all new submissions. Only one Agreement is required per submission.

CORRESPONDING AUTHOR

Name:	Nikki Posnack	
Department:	Sheikh Zayed Institute	
Institution:	Children's National Health System	
Title:	Assistant Professor	
Signature:		Date: 06/24/2019

Please submit a **signed** and **dated** copy of this license by one of the following three methods:

1. Upload an electronic version on the JoVE submission site
2. Fax the document to +1.866.381.2236
3. Mail the document to JoVE / Attn: JoVE Editorial / 1 Alewife Center #200 / Cambridge, MA 02140



Children's National Heart Institute
Sheikh Zayed Institute for Pediatric Surgical Innovation

Dear Dr. Xianyan Cao,

August 14, 2019

Enclosed you will find our revised manuscript, titled: **Optocardiography and electrophysiology studies of ex vivo Langendorff-perfused pig hearts**. We thank the reviewers and the Editor for their constructive comments to improve our manuscript for publication in the Journal of Visualized Experiments. As requested, comments are addressed point-by-point below and text modifications are highlighted in the revised track-changes manuscript.

General: As requested, edits were made to the manuscript layout, formatting, abbreviations, and commercial language.

Reviewer 1:

1. Lines 107-109: I like the idea of adding albumin to the perfusate..... The authors may consider elaborating on this a little bit in the Discussion, if metabolism is also concerned.

Thank you for the suggestion, we have included the following text in the Discussion (Lines 447-450): "During preparation and setup, we recommend adding albumin to the perfusate to maintain oncotic pressure and reduce edema (plus antifoam, if needed)"⁵⁶⁻⁵⁹. Moreover, perfusate containing albumin can also aid in metabolic studies that also require fatty acid-supplementation to the media^{60,61}."

2. Line 145: What is the BW range of pigs (or the heart sizes that fit the perfusion system described here)?

We have included this information in the revised manuscript (see Section 2.1): "Note: For this proof-of-principle study, juvenile Yorkshire pigs (14-42 days, n=18) were used that ranged from 2.5-10.5 kg body weight and 18-137 g heart weight (Figure 2)." Body weights and heart weights are in the new Figure 2.

3. Lines 184-187: What percentage of the hearts develop arrhythmias, at what time point, does a post-shock heart behave abnormally? Some discussion on this may help readers understand better the effect of defibrillation on the heart.

Thank you for this suggestion. In our experience, ~90% develop arrhythmias and require fibrillation. We have added this information (see Section 2.8): "In the presented study, 89% of preparations required defibrillation. After equilibration (~10 min), an average heart rate of 70±4.5 bpm was observed for juvenile piglet hearts and remained stable throughout the experiment (Figure 2).

4. Lines 201-202: The amount of dyes used here seemed quite low, comparing to what has been reported - <https://www.nature.com/articles/srep43217>. What is the SNR for both dyes following initial loading?

We have included additional information on how we prepare our dyes (Section 4.2, 4.3): "Prepare the voltage dye by dissolving 5 mg RH237 into 4 mL anhydrous DMSO. Dilute the dye aliquot with up to 5 mL of media and vortex. Slowly add RH237 (62.1 µg per 500 mL of perfusate) proximal to the aortic cannula. The myocardial tissue may be re-stained with RH237, if needed, throughout the duration of the experiment. Prepare the calcium dye by dissolving 1 mg of Rhod2-AM into 1 mL of anhydrous DMSO. Mix the dye with 50 µL of pluronic acid, place in a 37°C sonicating bath for up to 10 minutes, and then dilute with up to 5 mL of media. Slowly add the calcium dye (50 µg per 500 mL of perfusate) proximal to the aortic cannula. Note: To ensure uniform dye staining, dyes should be added slowly (>30 sec). Rhod-2AM takes up to 10 minutes to reach peak fluorescence, while RH237 stains the heart within a 1-2 minutes."

We have also included the SNR ranges for each dye following loading (Section 4.4): "Using the described dye loading, SNR ranges of ~42-86 and ~35-69 for voltage and calcium, respectively, can be expected." Using a larger dye concentration may further improve SNR.

5. Fig 1B: A ruler might be helpful to see the heart size.

Thank you for pointing this out – a scale bar is now included.

Reviewer 2:

1. Surprising to see a focus on, as stated in the text and shown in a photograph, pigs weighing as little as 2.2 kg and thus hearts of similar scale to that of rabbits. As the age and type of pig used was not provided, it is unclear if this is a neonatal animal or mini-pig variety.

The reviewer is correct. Since the lab is located in a Children's Hospital, our studies thus far have been largely focused on pediatric heart models. To clarify, we have reworded the introduction to emphasize the use of piglets, and have also included the body weights and heart weights for piglets used in this study (see Section 2: Heart Excision and Langendorff Perfusion): "Note: For this proof-of-principle study, juvenile Yorkshire pigs (14-42 days, n=18) were used that ranged from 2.5-10.5 kg body weight and 18-137 g heart weight (Figure 2)." We have also included the body weight and heart weight range in the new Figure 2.

We recently had the opportunity to successfully repeat our protocol using an isolated heart from a 36kg pig (348 g heart weight) that was procured for another laboratory's surgery study. We look forward to expanding our studies in the future.

2. Results are weighted heavily on the ECG recordings. It would be more pertinent to illustrate corresponding optical mapping signals.

We apologize for the confusion - we aimed to describe one comprehensive approach to study both (1) electrophysiology measurements and (2) optical mapping on the same heart. We usually perform these studies sequentially. To clarify our approach, we have separated the methodology section into two parts for (A) electrophysiological assessment (VERP, SNRT, WBCL, AVNERP) and (B) optical mapping studies of transmembrane voltage and intracellular calcium. We have included a citation on electrophysiological assessment (using similar parameters) for reference and comparison (Noszczyk-Nowak A, et al. Normal Values for Heart Electrophysiology Parameters of Healthy Swine Determined on Electrophysiology Study. Adv Clin Exp Med Wroclaw Medical University, 2016; 25:1249–1254.)

3. For signals from large animal hearts, they appear quite noisy.

To avoid confusion with other studies, we modified our data analysis and data representation (new Figure 4) to more closely compare our signals with those generated by others. As an example, Lee et al. 2016 doi:10.1038/snep43217 presents traces collected from a camera "configured to record 120×160 superpixels (4×4 binning mode; 4×4 pixels per superpixel) at 400 frames-per-second (fps)". This design results in a superpixel that is approximately 96x96 micron area in size – which is also comparable to studies published by the Efimov lab (Laughner, et al. 2012) that utilize a MiCMA Ultima with 100 micron size pixels. Both studies have an estimated projected resolution of approximately 1.5-4 mm tissue.

To help the reader compare between studies, we have cited both the Lee, et al 2016 and Laughner, et al 2012 papers, and generated a new figure 4 and figure 5 with signals collected from a similarly sized pixel area (15x15 pixels at 6.5 micron each= 97.5 raw superpixel). Figure 4 and Figure 5A,B displays signals without processing.

We have also included an action potential and calcium transient signal in Figure 5C – which includes temporal filtering (50 Hz) and normalization (max to min).

4. Probably a typo, but a flow rate of 340 ml/min was calculated for a heart from a 2.2Kg pig

Corrected. We have also included a range of flow rates for our studies (Section 2.6) "In our experience with juvenile piglet hearts, we observed an average initial flow rate of 184±17 mL/min that declined to 70±7.5 mL/min after perfusing with warmed media containing a mechanical uncoupler (20 mM BDM)." This data is also presented in the new Figure 2C.

5. Line 188: Flushing the heart was suggested here. This was presumably to flush the heart of residual blood (maybe also the cardioplegia?), please indicate this for clarity.

Modified (Section 2.9): “Flush the heart with at least 1 liter of media, without recirculating, to remove any residual blood and cardioplegia. Once the media runs clear through the heart, the circulating loop may be closed to recirculate perfusate.”

6. Line 192: It should be indicated that the ECG lead placements are not obligatory, but positions chosen were to obtain signals analogous to lead II.

Modified (Section 3.1): “To record a standard lead II ECG over the course of the study, attach a 29-gauge needle electrode to the ventricular epicardium near the apex, with another electrode in the right atrium. With the positive and negative inputs of a differential bioamplifier connected to the apex and right atrium respectively.”

7. Line 201 and 204: Normally, Ca dyes require a prolonged loading time to cross the cell membrane and diesterify. Here, a single bolus was injected. Therefore, it is presumed that the perfusate is being recirculated at this time and the loading is continuing through ? If loading depends upon recirculation, what is the total volume of perfusate and therefore concentration of the dye recirculating? Else, how slowly is the bolus introduced in to the perfusate?

We have included additional information on how we prepare our dyes (Section 4.2, 4.3): “Prepare the voltage dye by dissolving 5 mg RH237 into 4 mL anhydrous DMSO. Dilute the dye aliquot with up to 5 mL of media and vortex. Slowly add RH237 (62.1 μ g per 500 mL of perfusate) proximal to the aortic cannula. The myocardial tissue may be re-stained with RH237, if needed, throughout the duration of the experiment. Prepare the calcium dye by dissolving 1 mg of Rhod2-AM into 1 mL of anhydrous DMSO. Mix the dye with 50 μ L of pluronic acid, place in a 37°C sonicating bath for up to 10 minutes, and then dilute with up to 5 mL of media. Slowly add the calcium dye (50 μ g per 500 mL of perfusate) proximal to the aortic cannula. Note: To ensure uniform dye staining, dyes should be added slowly (>30 sec). Rhod-2AM takes up to 10 minutes to reach peak fluorescence, while RH237 stains the heart within a 1-2 minutes.”

Reviewer 3:

1. I suggest to provide a detailed schematic in Fig. 1 indicating the optical components. This will make it much easier to assemble to optical system. A note on the electrical triggering of the components could also be useful.

Thank you for the suggestion, more details on the components are presented in the new Figure 1. We manually triggered our light sources – and have noted that in the revised draft (Section 4.7)

2. Unfiltered raw data and a discussion of achievable fractional change and signal to noise ratio (SNR).

We have included unprocessed raw data in the new Figure 4, Figure 5A,B plotted as units of fractional change. To avoid confusion with other studies, we modified our data analysis and data representation (new Figure 4) to more closely compare our signals with those generated by others. As an example, Lee et al. 2016 doi:10.1038/snep43217 presents traces collected from a camera “configured to record 120×160 superpixels (4×4 binning mode; 4×4 pixels per superpixel) at 400 frames-per-second (fps)”. This design results in a superpixel that is approximately 96x96 micron area in size – which is also comparable to studies published by the Efimov lab (Laughner, et al. 2012) that utilize a MiCMA Ultima with 100 micron size pixels. Both studies have an estimated projected resolution of approximately 1.5-4 mm tissue.

To help the reader compare between studies, we have cited both the Lee, et al 2016 and Laughner, et al 2012 papers, and generated a new figure 4 and figure 5 with signals collected from a similarly sized pixel area (15x15 pixels at 6.5 micron each= 97.5 raw superpixel). Figure 4 and Figure 5A,B displays signals without processing.

We have also included an action potential and calcium transient signal in Figure 5C – which includes temporal filtering (50 Hz) and normalization (max to min). We have also included the SNR ranges for each dye following loading (Section 4.4): “Using the described dye loading, SNR ranges of ~42-86 and ~35-69 for voltage and calcium, respectively, can be expected.”

3. Although it might be obvious, it might be useful to emphasize that the illumination should be set to use the full well depth to provide maximum SNR.

We have noted (section 4.7) to “test the LED lights (525 nm, 1.4mW/mm²) prior to the start of imaging to ensure uniform and maximal epicardial illumination, as determined by the sensor well depth.”

4. The authors do not submerge the heart in a tissue bath ... I expect the glare points may occur on the heart's surface which could make the analysis of the data difficult.

Thank you, we have included this point in the text (Section 2.7) “Do not submerge the heart tissue, as it can impinge on cardiac imaging.” And the Discussion section (Lines 466-467): “To improve optical imaging endpoints, a hanging heart preparation limited the effect of glare that can occur with a submerged heart.”

5. Image registration is done with the software Metamorph... Could you provide additional information on the algorithm and the accuracy of the alignment?

*Per JOVE guidelines, we had to remove reference to Metamorph software in the text (still denoted in the Table 1 Materials). We have modified Section 4.6 to state: “Image alignment is best performed with the aid of software that can split the desired regions, overlay, and display a gray-scale subtraction or pseudo-color addition to highlight misalignment (see **Table 1** for software option).”*

6. I suggest to add a note of caution regarding the ongoing debate and indicate that the motion uncouplers blebbistatin may alter cardiac electrophysiology and may have an effect on defibrillation threshold.

Thank you for this suggestion – we have included the limitations of using mechanical uncouplers in the new Limitations section (Lines 483-492): “Another potential limitation to this study is the use of a mechanical uncoupler to reduce motion artifact during imaging. Blebbistatin has become the uncoupler of choice in cardiac imaging applications due to its minimal effects on ECG parameters, activation and refractory periods^{41,64,65}. BDM is a less expensive choice, which can be particularly important in large animal studies that require greater volumes of perfusate and mechanical uncoupler, but it is known to have a greater impact on potassium and calcium currents that can alter action potential morphology⁶⁶⁻⁶⁹. If BDM is used, note that APD shortening increases the hearts vulnerability to shock-induced arrhythmias⁷⁰. Conversely, the main limitation to using blebbistatin is its photosensitivity and phototoxicity, although alternative formulations that have reduced these effects⁷¹⁻⁷³.”

Reviewer #4:

1. Data processing, signal analysis and reconstruction of activation maps should be described as well.

This information is now included in the manuscript as several steps in section 6.2, see thresholding, spatial averaging, temporal filtering, drift removal.

2. The authors should show more optical mapping data, including (1) ventricular activation during spontaneous (sinus) rhythm, (2) ventricular activation at S2 extra stimulus (the shortest S1S2 interval used to measure VERP), (3) action potential duration distribution maps for spontaneous rhythm, S1S1 stimulation and for S2 extra stimulus, (4) calcium transient duration and calcium transient rise-up time distribution maps for spontaneous rhythm, S1S1 stimulation and for S2 extra stimulus, (5) action potential-calcium transient delay distribution map. All the maps should be accompanied by representative optical traces.

We apologize for the confusion - we aimed to describe one comprehensive approach to study both (1) electrophysiology measurements and (2) optical mapping on the same heart. We usually perform these studies sequentially. To clarify our approach, we have separated the methodology section into two parts for (1) electrophysiological assessment (VERP, SNRT, WBCL, AVNERP) and (2) optical mapping studies of transmembrane voltage and intracellular calcium. We have included a citation on electrophysiological assessment (using similar parameters) for reference and comparison (Noszczyk-Nowak A, et al. Normal Values for Heart Electrophysiology Parameters of Healthy Swine Determined on Electrophysiology Study. Adv Clin Exp Med Wroclaw Medical University, 2016; 25:1249–1254.)

As requested by the reviewer, we have included new data sets that depict spontaneous sinus rhythm (Figure 4), paced action potential duration map and activation time isochrones (Figure 5D), paced calcium transient duration map and activation time isochrones (Figure 5D), an overlay of action potential and calcium transient signals to show delay (Figure 5C), and an example of ventricular fibrillation (Figure 4).

3. The authors should also consider using different locations of the pacing electrode, including pacing from the right ventricle, apex and in the middle of the left ventricle. The latest should be used to assess conduction anisotropy, i.e., the ratio between the longitudinal and transversal conduction velocities.

Thank you for the suggestion. In the revised manuscript, we display action potentials and calcium transients from two regions of interest (RV and LV). We agree that it will be of interest to investigate regional differences in the tissue (RV, apex, LV) in future studies – but, these mechanistic experiments were not the focus of the current methodological study.

4. Did the authors observe any ventricular arrhythmias in their settings? It would be highly beneficial for readers to show an example of such ventricular tachyarrhythmia mapped and reconstructed for a few consecutive beats. This is important for those who will be using the presented experimental approach for studying ventricular arrhythmogenesis in a porcine model.

Thank you for the suggestion. We have included new data in figure 4 to display ventricular fibrillation.

5. The authors should indicate how stable was the heart rate (and, maybe, other EP parameters) over a course of the experiment, including that at baseline, after staining with fluorescent dyes, after immobilization with blebbistatin or BDM, and at the end of the experiment.

Unfortunately, our experimental approach did not include multiple EP studies across time. This will be interesting to investigate in the future. We have included new heart rate data at the beginning and end of study (new figure 2B) and changes in flow rate before and after perfusion with a mechanical uncoupler (new figure 2C).

6. Limitations of this experimental setup/protocol should be also described. In their experimental settings, the authors could image only a part of the heart (versus the entire ventricular surface at panoramic imaging).

As recommended, we have included a new limitations section which includes information on panoramic imaging, mechanical uncouplers and species differences (Lines 477-496).

7. It would be highly beneficial for readers to provide a schematic for the optical system. It is not clear from the text how the emission light was separated for voltage and calcium signals. Was a single camera used for a simultaneous recording of two signals?

Thank you – this is included in the new Figure 1, which depicts the configuration of the camera sensor, splitter and light paths.

8. Line 53-54: Not just this but also (and, probably, most important) because of affordable genetic manipulations available for rodents.

Modified, thank you for the suggestion.

9. Line 129: Please, specify what filter (brand, type) was used.

Per JOVE guidelines, we cannot describe brands in the text. However, filter properties are described in Section 4.5 and 4.7, and manufacturer details are provided in the Table of Materials.

10. Line 181-182: It would be helpful to measure a surface temperature to confirm that, in your experimental conditions, a heart surface indeed has the same temperature of 37 Celsius degree as perfusate.

Thank you for the suggestion. This information is now included (section 2.7): “Under full flow, we observe temperature ranges from 35C to 37C between the epicardium and endocardium, respectively.”

11. Line 192 and later: Please, describe how the pacing/ECG electrodes should be attached to the heart.

Modified (Section 3.1): “To record a standard lead II ECG over the course of the study, attach a 29-gauge needle electrode to the ventricular epicardium near the apex, with another electrode in the right atrium. With the positive and negative inputs of a differential bioamplifier connected to the apex and right atrium respectively.” Section 3.2: “Attach one bipolar stimulus electrode on the right atria, and a second bipolar stimulus electrode to the lateral left ventricle for pacing purposes.”

12. Line 196: Include an approximate normal baseline heart rate that should be achieved during heart stabilization and indicate a normal functioning of the heart after cannulation.

Thank you for the suggestion, this information is now included (Section 2.8) and shown in a new Figure 2: “In the presented study, 89% of preparations required defibrillation. After equilibration (~10 min), an average heart rate of 70 ± 4.5 bpm was observed for juvenile piglet hearts and remained stable throughout the experiment (Figure 2).”

13. Line 236: How many S1 pulses were applied before S2 extrastimulus? Were the same pulse parameters used for S2 as for S1?

We have included more details on the parameters we used for this study in Section 3.5: “Perform extrastimulus pacing using either an S1-S1 or S1-S2 pacing train, in the latter a train of 6-8 impulses (S1) was followed by a single impulse (S2)..... The same stimulation parameters are used for both S1 and S2 (1-2mA, 1 ms pulse width).”

Reviewer 5:

1. While this protocol may be of interest to other scientists, it is poorly described and contains several issues. The authors should consider adding information on the optical setup ... the external validity of this model ... human hearts.

Additional information on the optical setup is included, along with a new Figure 1 to show the configuration. We have added a reference to our previous manuscript that demonstrates the validity of our model (DOI: [10.1161/CIRCEP.119.007294](https://doi.org/10.1161/CIRCEP.119.007294) and DOI: [10.1101/651380](https://doi.org/10.1101/651380)). We have also included citations to cardiac models from other species (canine, human) in the Discussion section (Lines 442 – 444).

2. Figure 2 is very confusing. I would strongly recommend adding direct unipolar or bipolar atrial and ventricular electrogram recordings for this EP study rather than only ECG. You have to provide a more detailed overview and explanation of the described EP study..... Provide more detail on the reliable physiological range of SR, SNRT and all ERPs to validate the model.

Although our laboratory does not currently have an intracardiac catheter for programmed stimulation and recordings, we were able to easily measure SNRT, WBCL, AVNERP, and VERP using two pacing electrodes in conjunction with lead II electrocardiogram recordings. Additional details were included in Section 3.5. We have also included a reference to a previously published study on pig heart electrophysiology measurements (Noszczyk-Nowak A, et al. Normal Values for Heart Electrophysiology Parameters of Healthy Swine Determined on Electrophysiology Study. Adv Clin Exp Med Wroclaw Medical University, 2016; 25:1249–1254). Finally, we have noted in the Discussion section that alternatives are available (Lines 472-474): Although we describe the use of electrocardiograms to identify capture and loss of capture for various EP parameters, intracardiac catheters or bipolar recording electrodes can also be used.

In addition, expand on how programmed electrical stimulation is used to study cardiac dynamics by optical mapping. For example, I don't see how ventricular optical mapping can help assess SAN function?

The reviewer is correct, ventricular optical mapping does not help assess SAN function. We apologize for the confusion - we aimed to describe one comprehensive approach to study both (1) electrophysiology measurements and (2) optical mapping on the same heart. We usually perform these studies sequentially. To clarify our approach, we have separated the methodology section into two parts for (1) electrophysiological assessment (VERP, SNRT, WBCL, AVNERP) and (2) optical mapping studies of transmembrane voltage and intracellular calcium.

3. The authors exaggerated the clinical relevance of a pig model compared to other models. Pig cardiac anatomy is actually significantly different from that of a human....Please compare the efficacy of a pig model to other large animal models for the study of normal and abnormal cardiac function.

We have added text to the Introduction section which highlight the utility of using a pig model (Lines 74-82): “Indeed, previous studies have documented similarities in cardiac electrophysiology between humans and pigs, including similar ion currents⁸, action potential shape⁹, and responses to pharmacological testing¹⁰. Moreover, the porcine heart has contractile and relaxation kinetics that are more comparable to humans than either rodents or rabbits¹¹. Compared to a canine model, the porcine

coronary anatomy more closely resembles a human heart^{12,13} and is the model of choice for studies focused on heart development and/or congenital heart defects¹. Although there are differences between the pig and human heart⁹, these similarities make the porcine heart a valuable model for cardiovascular research¹⁴.”

We agree that each species has its own unique differences that have been thoroughly outlined by other reviews. In the Discussion section, we acknowledge that other laboratories may chose a different animal model to suit their specific research question: “Moreover, the described methodology can be modified and adapted for use with other cardiac models of interest (e.g., canine, human) depending on the specific research focus^{54,55}”

4. There are several labs (Efimov and Fedorov labs) that directly study with high-resolution optical mapping setups the physiology and pathophysiology of arrhythmias using explanted diseased and non-diseased human hearts. In line with this, the pig heart may only provide a higher throughput in comparison. Therefore the authors should address this in the manuscript.

We agree that the work on human heart specimens by Federov (atria), Janssen (trabeculae), Efimov (ventricular wedge prep, slices) and laizzo (whole heart MAP, pressure) is highly innovative. We see these approaches as complementary and not a limitation. Our methodology may prove useful to laboratories who do not have access to human tissue or who are interested in a specific parameter that is difficult to control with a rejected donor or diseased human hearts (example – sex and age differences). As this is an alternative, and not the focus of our study, we have briefly mentioned in the Discussion as stated above.

5. This protocol attempts to create a large animal model to characterize myocardial function; however, it is not made clear how large of a pig is used, and the manuscript references a 2.2 kg pig, which is not representative of a large animal but rather a small rabbit.

The reviewer is correct. Since the lab is located in a Children’s Hospital, our studies thus far have been largely focused on pediatric heart models. To avoid confusion, we have reworded the introduction to include reference to piglets, and have also included the body weight and heart weight size for piglets used in this study (see Section 2: Heart Excision and Langendorff Perfusion): “Note: For this proof-of-principle study, juvenile Yorkshire pigs (14-42 days, n=18) were used that ranged from 2.5-10.5 kg body weight and 18-137 g heart weight (Figure 2).” We have also included the body weight and heart weight range in the new Figure 2.

We recently had the opportunity to successfully repeat our protocol using an isolated heart from a 36kg pig (348 g heart weight) that was procured for another laboratory’s surgery study. We look forward to expanding our studies in the future.

6. Lines 178-180. The heart hangs from the aortic cannula and is not submerged in warm media, and as a result, a larger pig heart might not be maintained at an adequate temperature throughout the experiment.

Thank you for the suggestion. This information is now included (section 2.7): “Under full flow, we observe temperature ranges from 35C to 37C between the epicardium and endocardium, respectively.”

7. A bolus dose of calcium and voltage dye is introduced. However, a bolus should not be used when injecting dye. Instead, the dye should be warmed and slowly injected to avoid the harmful effects of concentrated dye which may lead to transient vasoconstriction, ischemia and arrhythmias. What was the process for diluting each dye and blebbistatin? DMSO? This needs to be described.

Additional details are provided in Section 4.1 – 4.3: “A mechanical uncoupler should be used to minimize motion artifacts during optical mapping and to avoid hypoxia^{6,37–39}. (-/-)Blebbistatin (5 μ M circulating concentration) may be added slowly as a bolus dose of 0.5 mM in 5mL perfusate (100x of final concentration)⁴⁰. Alternatively, BDM may be initially included in the perfusate media at a circulating concentration of 20 mM. Prepare the voltage dye by dissolving 5 mg RH237 into 4 mL anhydrous DMSO. Dilute the dye aliquot with up to 5 mL of media and vortex. Slowly add RH237 (62.1 μ g per 500 mL of perfusate) proximal to the aortic cannula. The myocardial tissue may be re-stained with RH237, if needed,

throughout the duration of the experiment. Prepare the calcium dye by dissolving 1 mg of Rhod2-AM into 1 mL of anhydrous DMSO. Mix the dye with 50 μ L of pluronic acid, place in a 37C sonicating bath for up to 10 minutes, and then dilute with up to 5 mL of media. Slowly add the calcium dye (50 μ g per 500 mL of perfusate) proximal to the aortic cannula. Note: To ensure uniform dye staining, dyes should be added slowly (>30 sec). Rhod-2AM takes up to 10 minutes to reach peak fluorescence, while RH237 stains the heart within a 1-2 minutes.”

8. Figure 3: Please provide direct validation of emission light separation for voltage and calcium signals. OAP and CaT should be overlap to show their morphology differences as well as delay 8-12 ms between upstrokes. Provide more detail on the reliable physiological range of OAP and CaT parameters (e.g. APD CaT 50 and 80), activation time and conduction velocities to validate the model.

References to the validation of emission light separation is now included (Section 4.5): “This configuration results in adequate emission light separation, as previously validated”^{43,44}. New Figure 5C depicts an optical action potential overlaid with a calcium transient, with time scale denoted. We have also included restitution curves to show action potential and calcium transient duration times at different pacing cycles (new Figure 5E,F) and included voltage and calcium activation maps (new Figure 5D).

9. Many classical refs are missing. For example, Lines 196-200 is missing a ref on Fedorov et al Heart Rhythm 2007 as first detailed application of blebbistatin for cardiac optical mapping experiments.

The reference to Fedorov’s blebbistatin paper has been added.

10. Refs 36 and 37 are identical

Corrected, thank you.

Thank you for your time and effort in reviewing our work.

Sincerely,



Nikki Gillum Posnack, Ph.D.
Assistant Professor
Children’s National Health System
Children’s Heart Institute
Sheikh Zayed for Pediatric Surgical Innovation
111 Michigan Avenue, NW, M7708
Washington, DC 20010
(202) 476-2475
nposnack@childrensnational.org

The George Washington University
School of Medicine and Health Sciences
Department of Pediatrics
Department of Biomedical Engineering
Department of Pharmacology & Physiology
2300 I Street, NW
Washington, DC 20037